

Applications of Machine Learning in Chemical and Biological Oceanography

Balamurugan Sadaippan¹, Preethiya Balakrishnan^{2, 3}, Vishal CR¹, Neethu T Vijayan¹, Mahendran Subramanian^{2, 4} and Mangesh U Gauns^{1*}

¹Plankton Laboratory, Biological Oceanography Division, CSIR-National Institute of Oceanography, Dona Paula, Goa-403004.

²Faraday-Fleming Laboratory, London, W148TL, United Kingdom.

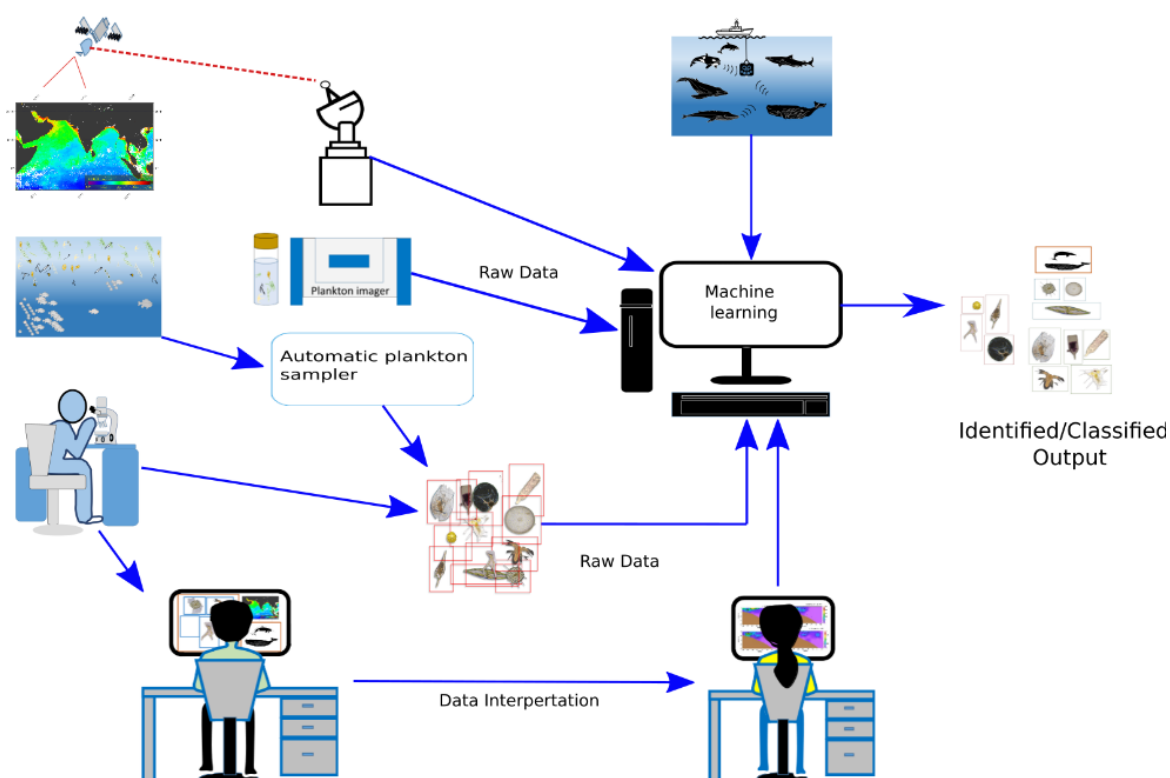
³University of London, London, WC1E 7HU, United Kingdom.

²Department of Computing, Imperial College, London, SW7 2AZ, United Kingdom.

Corresponding author: Mangesh Guans - email.id: gmangesh@nio.org

Abstract

Machine learning (ML) refers to computer algorithms that predict a meaningful output or categorise complex systems based on a large amount of data. ML applied in a variety of areas, including natural science, engineering, space exploration, and even gaming development. This article focused on the use of machine learning in the field of chemical and biological oceanography. In the prediction of global fixed nitrogen levels, partial carbon dioxide pressure, and other chemical properties, the application of ML is a promising tool. Machine learning is also utilised in the field of biological oceanography to detect planktonic forms from various images (i.e., microscopy, FlowCAM and video recorder), spectrometers, and other signal processing techniques. Moreover, ML successfully classified the mammals using their acoustics, detecting endangered mammalian and fish species in a specific environment. Most importantly, using environmental data, the ML proved to be an effective method for predicting hypoxic conditions and the harmful algal bloom events, an important measurement in terms of environmental monitoring. Furthermore, machine learning was used to construct a number of databases for various species that will be useful to other researchers, and the creation of new algorithms will help the marine research community better comprehend the chemistry and biology of the ocean.



Keywords: Machine learning, marine biology, marine chemistry, plankton, mammals, fish identification, Image analysis.

1. Introduction:

The ocean encloses complex ecosystems, each with a distinct physical, chemical, and geological composition supporting a vast spectrum of species. As the ocean covers 71% of the earth's surface, it supports more living organisms than the terrestrial habitats (Costello and Chaudhary, 2017). The earth biogeochemical cycle is heavily reliant on the ocean. Furthermore, it absorbs more than half of the carbon in the atmosphere. It also serves as the primary oxygen source. Due to its vast nature and complicated environment, continual monitoring is required to fully comprehend the ecosystem. As modern science progressed, additional research in the ocean environment was conducted on a local and global scale. Even the most distant sections of the Antarctic and Arctic regions are monitored. Decades of investigations yield a huge amount of data that reflect these ecosystems characteristics. It does become increasingly difficult to analyse big data using conventional numerical approaches.

Biological oceanography deals with understanding physical, chemical and other oceanography processes that influence the distribution and abundance of various types of marine life. Additionally deals with how living organisms like viruses, microbes, plankton and animals behave and interact with biogeochemical processes in the oceans (Lalli and Parsons, 1999). Furthermore, deals with how species adapt to environmental changes like the rise in temperature and pollution. Among the living organisms in the ocean, phytoplankton is the primary producer and plays an important role in the food web, as well as the biogeochemical cycle in the ocean (Kleppel and Burkart, 1995) and act as an indicator of pollution or eutrophication or climatic events (change in abundance and distribution) (Racault et al., 2014). Similarly, zooplankton play an important role in the marine food web, elementary cycle and vertical fluxes. Likewise, different eukaryotic organisms thrive in the ocean from fishes, turtles, dolphins, sharks and mammals like whales etc. All these organisms play a role in their ecosystem but are collectively facing difficulties due to climate change. Chemical Oceanography demonstrates the spatial and temporal distribution of elements, molecules, atoms and compounds, which are closely related to biological, physical and geological oceanography. It involves in the study of Carbon, nitrogen, sulfur and other element cycles. The ocean holds a larger portion of inorganic carbon than the atmosphere. The flow of chemicals in the ocean especially carbon depends on the earth's climate, the atmospheric CO₂ concentration increases rapidly due to the use of fossil fuel, which in turn increase the ocean carbon level (Johnson et al., 1992).

The discipline of machine learning (ML) is concerned with the use of computer algorithms to solve issues. It is a potential approach for allowing computers to assist people in analysing huge and

complicated data sets. ML is a type of statistical computing in which computers anticipate the outcome based on the input data (Yang, An, Zhou, & Hou, 2018). Furthermore, it is a subject that deals with constructing models, perform analysis, classification and prediction based on existing data (Kompore & Oani, 2014). ML techniques are frequently used to solve a range of large data issues, including image identification and classification, and extreme events in complex systems. In a complicated system, predicting and understanding unanticipated statistics is a difficult challenge (Qi, 2020). Machine Learning (ML) is the development of dynamic algorithms that can make data-driven choices. Because it can create a model from highly dimensional and nonlinear data with complicated relations and missing values, it also has an edge over traditional technique. In many aspects of the Earth system (land, ocean, and atmosphere), machine learning has proved to be quite beneficial (Ahmad, 2019).

ML is divided into several categories, including supervised, unsupervised, ensemble techniques, neural networks, deep learning and reinforcement learning. In supervised learning, algorithms require an external supervisor called training data. Human assistance usually provides precise input to get aimed output for prediction accuracy in training algorithms. In this, the algorithm first gets knowledge from the training data set to predict and classify the other data. In unsupervised learning algorithms, the computer program automatically searches for the feature or pattern from the given data and groups them into clusters without explicit programming. It uses the previously learned features to classify the new data. It doesn't need a supervisor or assistance for predicting the given data, so it is called unsupervised learning. Ensemble models are combining results from different models. It is an ensemble or collection of decision trees. It is also a versatile algorithm capable of performing both regression and classification. e.g., Random forest (RF).

Deep learning models are capable of focusing on the correct features on their own, needing little guidance. These models also partly fix the issue of dimensionality. The concept behind deep learning is to construct learning algorithms that imitate the human brain. Deep learning is a group of statistical systems gaining knowledge of strategies used to examine characteristic hierarchies, predominantly based on Artificial Neural Networks (ANNs). It has an input layer, a hidden layer, and an output layer. Such systems discover ways to make predictions via thinking about examples, typically without challenge-explicit programming. Back-propagation is a popular deep learning technique for performing supervised multi-layer perceptron training. Convolutional Neural Networks (CNN) consists of a sequence of layers like convolutional (input layer), pooling (reduce dimensions), and fully connected layer (Classification). CNN is a sort of feed-forward ANN in which the connectivity patterns between its neurons are influenced by the visual cortex organization of the animal. A computer understands an image or data and uses the layer to process the final class

score. In Reinforcement learning (RL) algorithms, the learning is based upon trial-and-error methods. RL uses various software to find the best behaviour or result. The decision is made based on action taken which gives more positive results.

Here, we focused on the application of ML approaches to understand big data associated with chemical and biological oceanography. Many researchers have utilised ML algorithms to address oceanography-related issues, such as determining phytoplankton dynamics, oceans remote sensing, habitat modelling and distribution, species identification, ocean monitoring and resource management.

2. Chemical oceanography

The ocean's carbon, micronutrients and macronutrients, are controlled by the physical, chemical biological and geological processes, driving the worldwide ocean biogeochemical cycles (Henley et al., 2020). Changes in biogeochemical processes in one place may have an effect on the global stage (Wang et al., 2020). The recent climate change issue, notably the rise in global temperature, has a significant impact on the biogeochemical cycle. As a result, getting a greater knowledge of the elements that drive change and measuring the impact is a difficult, but necessary task ahead. In this regard, we have discussed a few studies that employed machine learning to anticipate or estimate the elements in the ocean.

Gaussian Mixture Model, an unsupervised ML classifier can be used to understand the spatial variability of physical and biogeochemical properties in the intermediate and deep waters of Southern Ocean (SO) (Rosso et al. 2020). The ML, trained with Argo-based data (temperature and salinity) from 300 to 900 m depth, not only predicts the location and boundaries of the frontal zones but also organises them into five frontal zones. Also, predicts the water mass property variations relative to the zonal mean state. ML model also showed the variability is property dependent and may be twice as intense as the mean zone variability in intense eddy fields. Also, the ML model showed the intense variability in the intermediate and deep waters of the Subtropical Zone; in the Subantarctic Polar Frontal Zone, was closely related to the intense eddy variability that enhanced the convergence and mixing of the deep water with surface water.

2.1. Dissolved Oxygen (DO)

The concentration of DO in the ocean affects a variety of factors including seawater quality, global temperature control, ecosystems, biogeochemical cycling, ocean ventilation, and internal ocean circulation. The mixing of atmosphere-ocean interaction and a net amount of respiration of organic

matter in the water column control the ocean O₂ concentration (Emerson and Bushinsky 2015). Over the last century due to anthropogenic activities including excess fossil fuel use, the amount of O₂ concentration in the coastal and open ocean waters decreased (Breitburg et al., 2018). But there is no adequate data to find the seasonal and inter-annual variability on a global scale. In this section, we have discussed a few studies that employed the ML approach to assessing DO concentrations in various ocean realms.

Strong air-sea fluxes and oceanic instabilities are distinct features of the Southern Ocean (SO). The melting of polar ice caps due to global climate change has also affected the SO. As a result, research in these areas is of global importance. The DO concentration at 150 m depth of the SO was accurately estimated using Random Forest Regression (RFR) estimates with given temperature, salinity, location and time (Giglio et al. 2018). On validation with synthetic data from Southern Ocean State Estimate (SOSE), the RFR model performed well in estimating O₂ in most regions, while some boundary regions were difficult to predict. Additionally, RFR predicted that both the SOSE and World Ocean Atlas (WOA13) overestimate the yearly mean O₂ (at 150 m depth) in the SO both on a global and basin scale also, the model predicts that the SOSE may underestimate the O₂ annual cycle. The model also predicted a large regional bias in the east of Argentina. Overall, the RFR proved to be a better tool for understanding the annual mean O₂ and variability from the other sparse O₂ measurements. This RFR model may be useful to map other biogeochemical variables.

ML has shown to have better performance in the prediction of DO. However, the combination of different ML algorithms has its advantages, a combination of tree-based models and neural networks termed a Marine-Deep Jointly Informed Neural Network (M-DJINN) estimates the DO in the ocean (Wang et al., 2020). The M-DJINN use a zero-mean Gaussian distribution to predict the marine DO concentration. By choosing the number of trees and the maximum depth of trees the M-DJINN proved to be more efficient than DJINN in terms of computing time and prediction ability. M-DJINN performed better in terms of accuracy and convergence in predicting marine dissolved oxygen from the World Ocean Database 2013 (WOD13) dataset. Apart from the calculation time, M-DJINN decreases the mean squared error in predicting oxygen concentration to 17.6% (when the max tree depth was fixed at 10).

DO in the coastal regions is as important as DO in SO, as it supports the coastal economy. Apart from predicting the DO in water bodies, it is equally important to predict the hypoxic conditions well before it happens. Hypoxia, a low concentration of DO (less than 2 mg/l) in water bodies, mostly occurs in the estuaries and coastal waters. One of the major factors that cause mortality in

fishes and other aquatic organisms, in turn, alters the ecosystem community and influences the biogeochemical cycles (Diaz and Rosenberg, 2008). Recent climate and altered physical conditions aggravate hypoxia. So, early prediction of these conditions is essential for environmental management. However, the accurate prediction of DO spatial-temporal variation and hypoxia is still a difficult task even with advanced numerical methods. ML models like RFR and Support vector regression (SVR) with little training datasets accurately predicted the offshore and nearshore DO concentration (Valera et al., 2020). Both the models with measured DO concentration from offshore, nearshore and measured input parameters accurately reproduced the DO concentration. Among the models, RFR performed better than SVR (difficult to tune and took longer training time). The model showed high accuracy in predicting the DO value with training data from the same site but perform moderately in predicting the DO in one site with training data from another site. The model also has some abilities like, correcting the missing data in time series datasets and detecting coastal hypoxic conditions directly or indirectly. Future iterations of such ML models may produce an accurate real-time forecast of hypoxic events. Apart from the simple ML algorithms, neural networks were also used to estimate or predict the DO concentration in the coastal environment. The spatial-temporal variations of DO and hypoxic conditions in the Chesapeake Bay, USA were predicted using a neural network (Yu et al., 2020). Where, the data were processed in three major steps i.e., empirical orthogonal functions analysis, automatic selection of forcing transformation, and a neural network. The model has high accuracy with external forcing as model inputs rather than the in-situ measurements. This model proved to be useful in coastal systems which are systematically monitored.

Even with different machine learning algorithms, accurate forecasting of DO is still challenging. The nonstationary and extreme volatility nature of the DO make it difficult to predict. Even with predictors and applying different ensemble models the accurate forecasting of DO is a challenging task. The complexity of using multiple factors affecting DO and applying different ensemble models were overcome by using the Grey Relational (GR) degree method, Empirical Wavelet Transform (EWT) and multi-model optimization ensemble optimization ensemble. Among the models, a novel hybrid model MF-RNNs-EWT-BEGOE based on the weightage obtained by particle swarm optimization and gravitational search algorithm had better prediction accuracy (Liu et al., 2021). The model showed to be superior with excellent accuracy in forecasting DO also, the model has the ability to predict the trend and enable humans to have better management decisions.

2.2. Carbon (C)

The oceanic uptake of CO₂ caused ocean acidification (increased by ~0.1 pH units) which may lead to biodiversity loss (Raven et al., 2005). The ocean's role in the carbon cycle and spatial heterogeneity of CO₂ flux can be determined by measuring the sea-surface partial pressure of carbon dioxide (pCO₂), an essential parameter in quantifying air-sea CO₂ flux. So, it is important to understand the oceanic uptake and dynamics of the pCO₂. The pCO₂ was estimated by shipboard (*In situ*), Agro floats, and satellite image datasets. Satellite data-based estimation was found to be a promising field which required less time and cost. The practical difficulty in measuring pCO₂ from satellite data is that multiple environmental factors control the pCO₂. Early, pCO₂ was estimated using regression and multiple regression (Stephens et al., 1995; Sarma, 2003; Ono et al., 2004; Jamet et al., 2007; Sarma et al., 2006; Zhu et al., 2009; Chen et al., 2011; Marrec et al., 2015) from the satellite data like Sea Surface Temperature (SST), Sea Surface Salinity (SSS), Chlorophyll-a (Chl-a) concentration, downwelling of irradiance (Kd), wind and Mixed Layer Depth (MLD). These analyses were not able to accurately estimate pCO₂ in large oceanic regions. Also, features (predictors) play an important role in determining the pCO₂, so selecting parameters from the satellite data for estimating pCO₂ was important. Here we discussed a few studies that used different ML algorithms and parameters to measure the pCO₂ in the coastal and open oceans around the globe.

Alternate to the statistical model, a Self-Organised Map (SOM), a neural network, successfully mapped the pCO₂ in the Atlantic subpolar gyre with latitude, longitude and SST (Lefèvre et al., 2005). SOM also predicted the remaining data with better accuracy than linear regression, and an average of 0.15 Gt-C yr⁻¹ sink was estimated from 1995 – 1997 (Lefèvre et al., 2005). Later, SST and Chl-a SOM mapped a basin-wide pCO₂ in the Northern Atlantic (RMSE of 19.0 µatm a perfect speculative interpolation) with gaps in remote sensing data and performed better when climatological SST and Chl-a were filled in the gaps (Friedrich and Oschlies, 2009a). Due to the large gap in remote sensing data, Friedrich and Oschlies (2009b) mapped the pCO₂ in the Gulf of Mexico (basin-wide) using Voluntary Observing Ship (VOS) observation and Agro float data (SST and Chl-a). Notably, the use of Agro data reduced the RMSE in predicting the annual cycle pCO₂ by 40% (RMSE of 15.9 µatm). Likewise, in the Northern Atlantic basin, the SOM mapped the pCO₂ and provided the non-linear relationships between marine pCO₂ and three biogeochemical parameters (Telszewski et al., 2009). Satellite-derived Chl-a and SST along with MLD SOM had RMSE of 11.6 µatm and estimated pCO₂ at a range of 208 to 437 µatm similar to the in-situ measurements (Telszewski et al., 2009). Similarly, with SST, Chl-a and wind stress, SOM estimated the pCO₂ for the entire west coast of the North American Pacific and identified 13

biogeochemical sub-regions. A unique parameterisation model was applied for each sub-region, which resulted in the estimation of $p\text{CO}_2$ with RMSE ranging between 6.6 to 65.0 μatm (Hales et al., 2012). Mapping $p\text{CO}_2$ on a global scale remains challenging as the model created for one region will not perform well for other regions. Moreover, the addition of SSS in training data improved the performance of SOM in estimating $p\text{CO}_2$ in the North Pacific Ocean. The SOM estimated values were paired with the in-situ measurement and accurately reproduced the $p\text{CO}_2$ values in several time-series locations. Similarly, monthly $p\text{CO}_2$ estimation by SOM was similar to the Lamont-Doherty Earth Observatory measurements (Nakaoka et al., 2013).

Likewise, a Feed Forward Neural Network (FFNN) estimated the $p\text{CO}_2$ reasonably agreed with the in-situ measurement with the same parameters SST, Chl-a, latitude and longitude. The monthly variations of $p\text{CO}_2$ with RMSE of ~ 6 μatm were measured using MODIS-Chl-a and SST data. Also, NN estimated the offshore and onshore $p\text{CO}_2$ (13.0 μatm and 12.05 μatm respectively) with some uncertainties associated with MODIS data and NN (Jo et al., 2012). A dataset using satellite images was created using FFNN with all the necessary parameters, which helped to estimate the global carbon budget (Zeng et al., 2015). With a dataset similar to Zeng et al. (2015), the comparative analysis showed SVM a better performance in mapping global surface $p\text{CO}_2$ followed by FFNN, which took a long time to train. Whereas SOM was the least, albeit SOM had the advantage of fast prediction by training and re-labelling, it depends on data scaling, which may cause nonsense predictions (Zeng et al., (2017)). In the case of the tropical Atlantic Ocean with the same type of satellite parameters (SST, Chl-a and SSS), the FFNN model has better prediction accuracy (RMSE of 8.7 μatm) than the linear regression (Moussa et al., 2016). Also, the regression tree algorithms showed the satellite drove $p\text{CO}_2$ values (based on Chl-a, SST and dissolved organic matter) correlated (r^2 of 0.827 and prediction error 31.7 μatm) well with ship-based $p\text{CO}_2$ measurement. Moreover, $p\text{CO}_2$ predicted with satellite-derived salinity was coherent with shipboard measurements. The regression tree model also determined the seasonal air-sea flux of CO_2 , which was similar to biogeochemical models. The tree also predicted that the regional environmental parameters influence the regional spatial distribution patterns of $p\text{CO}_2$ (Lohrenz et al., 2018).

Moreover, the global ocean $p\text{CO}_2$ was estimated by FFNN with climatological and Surface Ocean CO_2 Atlas (SOCAT) with predictors like SST, SSS, Chl-a, MLD, and sea surface height, latitude and longitude. Also, the NN predicted the seasonal and interannual variability in the global ocean, where large regions with poor coverage differed in $p\text{CO}_2$ patterns (Denvil-Sommer et al., 2019). The application difficulties of a model created in one region to map the $p\text{CO}_2$ of another region were solved by a Random Forest-Based Regression Ensemble (RFRE) (Chen et al., 2019). Different ML models were trained and tested with a dataset consisting of field-measured $p\text{CO}_2$ data and

satellite data like SST, SSS, Chl-a and Kd. Among the ML models, an RFRE showed better performance with high accuracy (~1 km spatial resolution), and less root mean square difference (RMSD) of 9.1 μatm . The model estimated the pCO_2 at a range of 145–550 μatm in most of the Gulf of Mexico regions, and the uncertainty of SST and SSS was found to be highly sensitive compared to the Chl-a and Kd in estimating pCO_2 . The robustness of the RFRE approach performed well when compared with the locally trained model in estimating the pCO_2 in the Gulf of Maine. This indicates that the RFRE may be applied to other regions with adequate *in situ* data (Chen et al., 2019). The Cubist model identified the spatial and temporal distributions of pCO_2 in the Gulf of Mexico region, which showed the seasonal CO_2 flux in the region closely related to the change in environmental parameters. Cubist also performed better than most ML algorithms with an RMSE of 8.42 μatm , where SST, SSS and Chl-a act as essential variables in estimating pCO_2 . Also, the model divides the Gulf of Mexico into six sub-regions based on the distribution of pCO_2 (Fu et al., 2020). As predictors play a vital role in the estimation of pCO_2 , the FFNN model was used to select the predictors based on the mean absolute error from the 11 biogeochemical regions derived by the SOM. Where FFNN had high precision (with region-specific predictors) in estimating global monthly pCO_2 with satellite data ($1^\circ \times 1^\circ$ resolution), also reduced the mean absolute error to 11.32 μatm and RMSE to 17.99 μatm (Zhong et al., 2022).

Other than pCO_2 , the global distribution of total organic carbon (TOC) in the seafloor sediment was determined by the K-Nearest neighbour (KNN) algorithm (Lee et al., 2019). Based on the estimated geochemical and geophysical properties model, about 87 ± 43 gigatons (Gt) of organic carbon are stored in the upper 5 cm of the seafloor.

2.3. Nitrogen (N_2) and other chemicals

Fixed nitrogen is a vital nutrient for all life on earth, and minor geographical variations in nitrogen bioavailability cause huge disparities in primary production, ecosystem dynamics, and biogeochemical cycles (Voss et al., 2013). The balance between denitrification, which occurs primarily in oxygen minimum zones (OMZs), and N_2 fixation by diazotrophs, which occurs primarily in (sub)tropical gyres, determines the fixed N_2 forms in the oceans (Deutsch et al., 2007; Naafs et al., 2019). The recent estimate of worldwide marine fixation N_2 ranged from less than 100 Tg N/year to more than 200 Tg N/year (Luo et al., 2012). Trichodesmium and unicellular cyanobacteria group-A (UCYN-A) diazotrophs and non-cyanobacterial diazotrophs have been shown to contribute considerably to N_2 fixation as per the recent studies (Bombar et al., 2016; Delmont et al., 2018). According to statistical algorithms, surface solar radiation and subsurface

minimum oxygen are critical factors in the geographic distribution of marine fixed N_2 (Luo et al., 2014). Also, it does not clearly explain the decrease of nitrogen fixation when the subsurface minimum dissolved oxygen level is higher than $\sim 150 \mu M$. Multiple linear regression estimated the global integrated nitrogen fixation was at 74 Tg N/y with error ranging between 51–110 Tg N/y (Luo et al., 2014). Similar results were predicted by the RF and SVR model (global N_2 fixation at a range of 68–90 Tg N/year) based on environmental and biological factors. However, both models showed geographic differences in the N_2 fixation, which was different from the other ocean model predictions. This may occur due to the underestimation of diazotrophs (widely distributed and diverse organisms) concentration in the global ocean. Predicting global N_2 fixation is still a challenging task. Measuring methods such as physiological investigations, satellite estimates, extended observations in under-sampled locations, and advanced ML algorithms will solve this problem.

Likewise, ML addressed the limitation in estimating sedimentary carbonate on the ocean floor and its complex chemistry. The global ocean floor sedimentary carbonate estimation measured the carbonate in the individual site and extrapolated it using an inverse distance weighted technique subjected to a high error rate. To overcome the limitation of datasets, Bradbury & Turchyn (2019) used a different ML model to estimate sedimentary carbonate. ML-classification tree (based on the Recursive Partitioning (RPART) approach) showed an accuracy of 73%. The model was trained with oceanic physical and chemical properties, including bathymetry, temperature, water depth, distance from shore, tracers of primary production, and data from the global database. ML estimated the total amount of sedimentary carbonate formation ($1.35 \pm 0.5 \text{ mol C/yr}$), which was lower than the previous estimation. Also, ML predicted that 77% of sedimentary carbonate today is mainly driven by anaerobic methane oxidation followed by organoclastic sulphate reduction.

Random Forest ensemble model predicted the global ocean surface bromoform and dibromomethane. These halogenated compounds have a short life and affect ozone in the atmosphere. A data-driven ML algorithm considering the ocean and atmosphere physical parameters along with the biogeochemical factors estimated a global ocean surface emission of 385 and 54 Gg Br per year bromoform and dibromomethane, respectively (Wang et al., 2019). Likewise, the sea surface methane disequilibrium (ΔCH_4) distribution was mapped by Artificial Neural Networks (ANN) and Random Regression Forests (RRF). Both the models successfully predicted local and global spatial patterns, magnitude, and variation of ΔCH_4 and estimated the global diffusive CH_4 flux of 2–6 Tg CH_4 per year from the ocean to the atmosphere. Also, the model showed that the flux was high in near-shore regions where CH_4 releases to the atmosphere before oxidation.

3. Biological oceanography

3.1. Plankton

Phytoplankton is a vital component of the marine environment as they play a crucial role in the biogeochemical cycle. It is a biological criterion for determining the quality of the ocean. Identifying phytoplankton is essential for environmental monitoring, climate change monitoring, and water quality evaluation. Also, understanding the marine plankton ecosystem requires identifying and categorising them to assess their diversity and abundance. On the other hand, phytoplankton species identification is difficult due to their variability and ambiguity, as there are thousands of micro and pico-plankton species and an imbalance in the distribution of various taxa. Phytoplankton is recognised via imagery and spectrophotometry. Especially identifying phytoplankton using images is complicated because of the high variation and image quality. Herewith, we have discussed a few studies in which machine learning algorithms were used for various tasks, including identification, classification, and database creation.

3.1.1. Image based classification of phytoplankton

Manual analysis of the imagery captured by underwater camera systems is a feasible solution. However, the main difficulties in image classification are image quality, illumination, background noise, angle of the plankton in the image, and deformed objects. Automated image classification using machine learning tools is an alternative to the manual approach. The classification of phytoplankton using ML started in the early 1990s. The microscopic images were converted into two-dimensional spectral frequency and classified by pattern recognising algorithm (Schlimpert et al. 1980). Later, with pre-processed microscopic images (with Fourier transformation and edge detection), two neural networks and two classical statistical techniques identified 23 dinoflagellates from the images. Among them, a radial basis network outperformed others with 83% accuracy (human 85% accuracy). Moreover, with a combination of Fourier feature, moment invariants and grey-scale morphological granulometric, the Learning Vector Quantization classifier (LVQ) classified diatoms and other five planktons with an accuracy of 95%. The LVQ was trained and tested with ~ 2000 images from the Video Plankton Recorder (VPR) (Tang et al., 1998). However, the same LVQ with the same features applied to an actual image dataset from the VPR system classified *Chaetoceros socialis* with an accuracy of 86% (true positives). Nevertheless, the overall accuracy for seven taxa (e.g., Copepod, Pteropods, Pseudocalanus, Diatoms) was only 60-70% (Davis et al., 2004). Also, classification error was high for low abundant taxa. Using a co-occurrence matrix and SVM considerably reduced the error rate for low abundant taxa (more than 50% for *Chaetoceros socialis*) (Hu and Davis, 2005).

Apart from the camera and scanner images, phytoplanktons were identified from the Shadow Image Particle Profiling Evaluation Recorder (SIPPER). The main problem with SIPPER was that many images lacked distinct outlines. With extracted general and domain-specific features, SVM classified diatoms with an accuracy of 79% (with only 64 samples in the training set). The model classified the *Trichodesmium* with an accuracy of 72.5% in both experiments with 29 and 15 features (Luo et al. 2004). A probability value was introduced to evaluate the SVM accuracy, and SVM outperformed the C4.5 decision tree and a cascade correlation neural network performance with two different datasets (known plankton images and images with unidentified particles). Also, with a minimal dataset, single SVM outperformed ensembles of decision trees created by bagging and random forests. However, the model struggled to identify unidentified particles in large image datasets (Luo et al. 2004). However, Sosik & Olson (2007) developed a model by combining the feature selection algorithm (Greedy Feature Flip Algorithm (G-flip)) and SVM to identify and measure the abundance of phytoplankton based on the taxonomy from the images taken by custom-built submersible FlowCytobot. A total of 22-category training sets with 131 features were selected from 210 features by G-flip, and SVM was trained with these features, which had an overall accuracy of 88% in classifying independent test sets and 68% to 99% accuracy for individual class categories. Also, cross-validated with two-month time-series data from Woods Hole Harbor showing unbiased results concerning manual estimation (random sampling). The model also gave the temporal resolution of phytoplankton abundance and seasonal plankton variability (Sosik & Olson, 2007).

FlowCAM automatic plankton identifier was developed, which uses SVM to classify plankton from images. Even though this automated FlowCAM is an alternate method for manual microscopy, some aspects must be improved to analyse field samples. The classification accuracy of SVM was improved by up to 86% when the images of non-living objects were eliminated by an automated step (Alvarez et al., 2012). SVM also identified the misestimation of the biovolume of chain-forming diatoms by the current automated method when the biomass of chain-forming diatoms was more than 20% in the sample (estimated using > 500 samples). Such classification methods can be used to assign taxon and simultaneously estimate the biovolume of plankton. Moreover, a minimal difference was observed while comparing the manual estimation (Alvarez et al., 2014). This slight difference was due to preservation and inaccuracy associated with the automated classification. However, these two approaches had similar results while identifying the seasonal variations in the abundance, biomass, and diversity of plankton in the Cantabrian Sea time series data (Alvarez et al., 2014). Then different features like general and robust were combined by non-linear Multiple Kernel Learning (MKL), and the use of three kernels (linear, polynomial and Gaussian kernel functions)

showed high recall and precision (90% and 9.91%, respectively) for WHOI dataset from Woods Hole Harbor water. Also, it performed better than one kernel and SVM. The only limitation of this model is that it has low efficiency with extremely imbalanced datasets (Zheng et al., 2017).

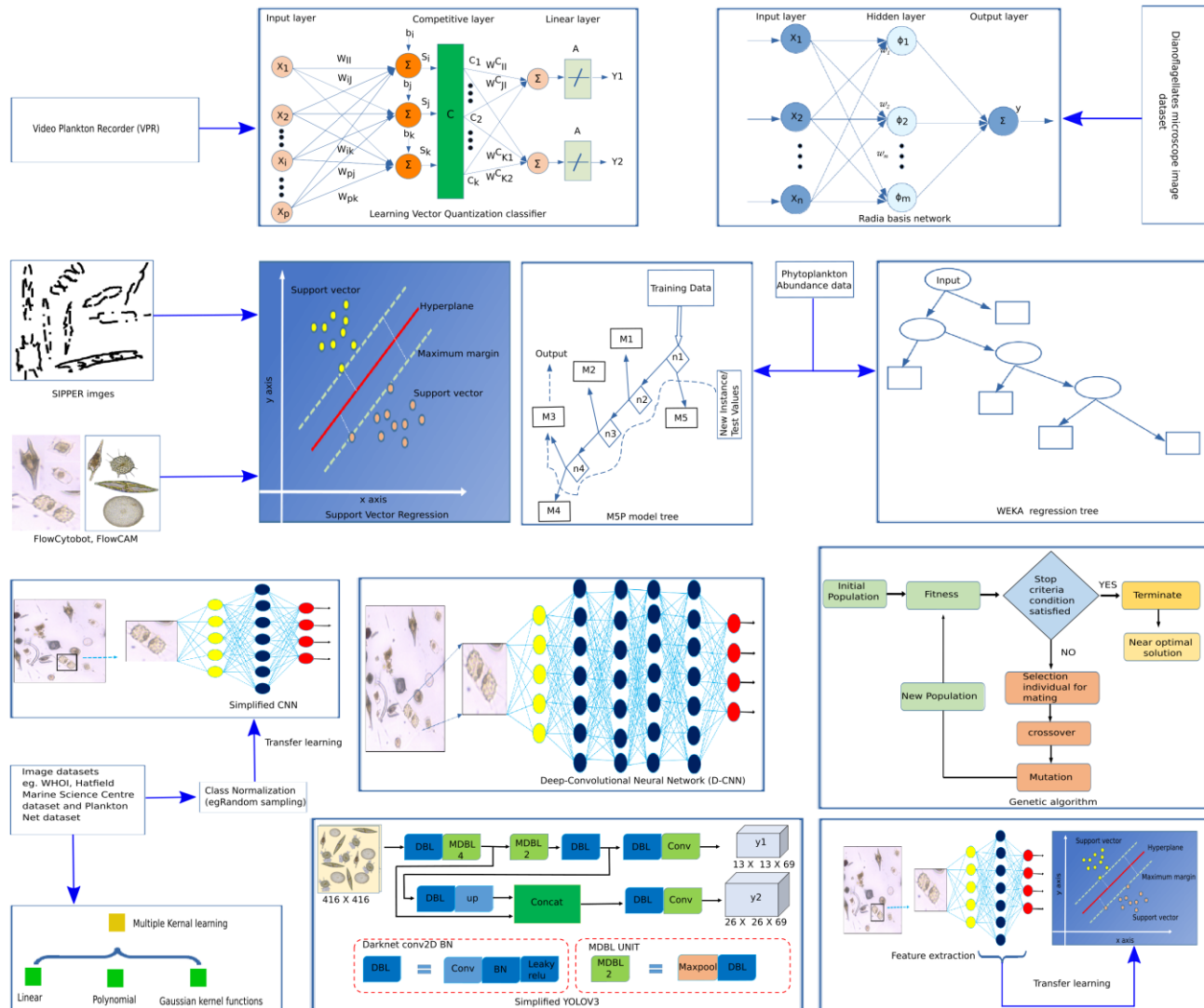


Figure 1. Use of ML algorithms to identify, predict, and classify marine phytoplankton from images.

Few studies have used neural networks to classify plankton. A Deep Convolutional Neural Network (D-CNN) using rotational and translational symmetry features successfully classified plankton with high accuracy and effectiveness from the plankton set 1.0 image dataset. The two conditions were implemented in CNN layers, i.e., to ensure each convolutional layer can learn complex image patterns and the receptive field of the top layer should be no greater than the image region. In addition, the inception layer was developed to handle images of various sizes (Py et al., 2016). Most datasets, like the WHOI-Plankton dataset, had the class imbalance problem, leading most models to

classify only the major classes and neglect the minor class during classification. The transfer learning-based CNN and the class normalisation function solved this problem. Where class normalised dataset was created by reducing the large-sized classes by random sampling, and the CIFAR10 CNN model was trained with the normalised dataset. To reflect the actual data size, transfer learning was applied to the CNN trained with normalised data by re-training with the original dataset, which improved the class imbalance problem and class population bias in classifying planktons. Also, CNN with normalised data and transfer learning had better overall accuracy than CNN with different data augmentation with transfer learning and CNN without transfer learning (Lee et al., 2016).

Also, a combination of algorithms trained to extract features from nonplankton images and classifiers re-trained with plankton images showed high performance in classifying plankton. This method is an advancement in CNN that provides better or comparable results (Orenstein & Beijbom 2017). Similarly, Rodrigues et al. (2018) applied the CNN-based transfer learning approach to extract the features from the openly available plankton image dataset and used SVM to classify planktons, which had good accuracy. This showed the transfer learning approach's effectiveness in coping with the large scale and high variable plankton images dataset. Also, the usefulness of CNN-based feature extraction as an alternative for regular hand-picked features is to estimate the commonly available planktons in the water samples. Where the ResNets pre-trained with the ImageNet dataset were used to obtain features, the model with these deep features better estimated the commonly occurring plankton class in the water sample (Gonzalez et al., 2019).

Apart from the extraction and transfer learning, a Deep Convolutional Neural Network (DCNN) was used to reconstruct the phase contrast image. A portable flow cytometer with coherent lens-free holographic microscopy captures diffraction patterns of objects that flow through the microfluidic channel at a rate of 1000ml/h. DL phase-recovery reconstructed the diffraction patterns, and the images were reconstructed in real time. This device showed high efficiency in capturing images from the ocean samples and showed similar results to the California Department of Public Health in measuring the abundance of toxic plankton *Pseudo-nitzschia* in six Los Angeles public beaches. This portable imaging flow cytometer may be used for continuous economic and portable monitoring (Gorocs et al., 2018). Similarly, CNN identified six planktic foraminifera with better precision and recall accuracy (80%). The CNN trained with database containing light microscopic images of six pale-oceanographic important planktic foraminifera (at 16 different illumination angles) had better performance than human beginners and experts. This automatic identification may lead to the development of an automatic robotic system to identify foraminifera and reduce the

time, which allows human experts to focus on the morphotypes or intergrades. Also, this method aids humans in gaining more profound knowledge of foraminifera taxonomy in less time (Mitra et al., 2019).

Another functional adaption in CNN was the combination of several fine-tuning CNN models that were trained to different strategies and proved to have better performance than a single CNN in classifying plankton (from 3 plankton and 2 coral datasets). Even though the stand-alone DenseNet was found to be the best model for the target datasets, the ensemble model has considerable improvements. Also, the final proposed ensemble consisting of only 11 classifiers (the number of classifiers was also reduced using feature selection) performed better (Lumini et al., 2020). CNN also identified the taxonomy of diverse morphological diatoms from the image datasets assembled from two Southern Ocean expeditions. The CNN performed well in background masking, adjusting data set size and possible changes in image classification performance. The old CNN architect model, VGG16, had better performance and generalising ability from the given image dataset, which was further improved after background masking. Also, CNN showed high performance in identifying the non-domain specific image when the top layer of CNN architect was alone trained extensively.

Likewise, Li et al. (2020) introduced a new phytoplankton microscopic image dataset (PMID2019), which contains 10 819 phytoplankton microscopic images of 24 different classes. The dataset was created using the dead cells, and Cycle-Consistent Adversarial Networks (cycle-GAN) were utilised to generate the corresponding living phytoplankton cell. Also, a few live cell images (only 217 images including 10 different categories) were included in the dataset. The database was tested with different ML algorithms; among them, Fast R-CNN has better accuracy for predicting the location and class of plankton in the images. The PMID2019 database assesses ML algorithms' performance that detects plankton from the image.

3.1.2. Estimation of ocean chlorophyll-a from satellite data

Microalgae, especially phytoplanktons, dominate the upper sunlight zone of the ocean, act as the primary source of the oceanic food web and fix carbon via photosynthesis (Sabine et al., 2004; Falkowski, 2012). This phytoplankton has a pigment called Chlorophyll-a (Chl-a), which involves photosynthesis and measuring Chl-a as an essential parameter in assessing water quality. Along with Chl-a, suspended particles and coloured dissolved organic matter (CDOM) in the surface water can be measured using remote sensing. The recent development of sensors (Moderate Resolution Spectroradiometer (MODIS), Sea-viewing Wide Field-of-view Sensor statistics (SeaWiFS), and

Medium Resolution Imaging Spectrometer sensors (MERIS) and different retrieval algorithms were used to estimate the Chl-a concentration from remote sensing data. However, the accurate measurement of Chl-a from satellite data is still challenging. Here, we have discussed a few studies implementing ML algorithms to estimate the Chl-a from remote sensing data.

The accurate Estimation of Chl-a and monitoring of the coastal environment is still challenging even with three decades of satellite observation. The coastal water quality is influenced by many factors like inputs from inland and coastal circulation. The simple numerical methods could not accurately estimate the water quality because different factors like suspended particulate matter (SPMs) and CDOM affect the spectral response. However, SVR algorithms overcome these limitations and estimate the Chl-a and SPMs concentrations in the surface waters of the west coast of South Korea (Kim et al., 2014). SVR has shown better prediction accuracy than Random Forest (RF) and Cubist, with R^2 values of 0.91 and 0.98 for Chl-a and SPMs, respectively. Geostationary Ocean Colour Imager (GOCI) satellite data and the field measurements data (as reference) were used for training and testing. Where SVR showed the ratio of band 2 to band 4, and bands 6 and 5 were the critical variables in predicting the Chl-a and SPMs concentration when GOCI-derived radiance data were used.

Similarly, SVR successfully estimated the surface global ocean Chl-a concentration from the NASA bio-Optical Marine Algorithm Data set (NOMAD) (Hu et al., 2020). SVR reduces the image noise and improves the cross-sensor consistency; it also produces consistent results with different sensors (SeaWiFS, MODISA, and MERIS) and performs better than the band-ratio OC x approaches (evaluation with various sensor data). Even though the SVR performance was statistically slightly less than the empirical colour index (CI) algorithms for $\text{Chl} < 0.25 \text{ mg m}^{-3}$ (Hu et al., 2012). The SVR model showed extended applicability to international waters, from the CIs 0.01-0.25 mg m^{-3} (about 75% of the global oceans) to its 0.01-1 mg m^{-3} (96% of the global ocean). Also, compared to the NASA hybrid Ocean algorithm (OCI), SVR was simple and avoided the complexity of mixing two algorithms.

However, Extra tree, a deep learning model, successfully measured the Chl-a concentration from the sea surface reflectance data over West Africa (Diouf & Seck, 2019). The ESA Ocean Colour Climate Change Initiative satellite sensor data was used as a training dataset, whereas the MODIS sensor dataset was used to validate the model. The Extra tree show high accuracy (96.46%) and low mean absolute error (0.07 mg/m^{-3}), and the model performed well with mixed or single sensor data. Also, the estimated Chl-a values by the Extra tree model were consistent with upwelling

phenomena observed in this area (Diouf & Seck, 2019). However, using Bayesian maximum entropy (BME) and SVR improved Chl-a estimation from satellite reflectance data by reducing the non-negligible uncertainties (He et al., 2019). In the initial model building step, SVR performed well with high accuracy than other ML algorithms in estimating the Chl-a concentration from MODIS Remote sensing reflectance (R_{rs}) at 412, 443, 488, 531 and 678 nm data with R^2 value varied between 0.708 to 0.907 for training and validation respectively. Then this SVR estimated Chl-a concentration was processed using BME with the incorporation of inherent spatiotemporal dependency of physical Chl-a distribution, reducing 50% of the mean uncertainties.

The BME/SVR also estimated the daily mean Chl-a concentration, which varied between 1.663 to 3.343 mg/m³ (He et al., 2019). Besides the SVR and deep learning models, NN was also used to estimate the Chl-a from satellite reflectance data. Among the tested ML algorithms, ANN performed better in estimating the Chl-a, suspended solids and turbidity from the Landsat reflectance data. Moreover, compared to standard Case-2 Regional/Coast Colour" (C2RCC), ANN had high accuracy in estimating Chl-a from satellite (91% accuracy with a low RMSE value of 2.7 µg/L) as well as from the *in situ* reflectance datasets (89%) (Hafeez et al., 2019). Likely, CNN has also been used to estimate the spatial and temporal distributions of Chl-a in the Korean bay (Jin et al., 2021). Two CNN models were built (Which use different dimensions of satellite images), trained and tested with satellite colour images data (Chl-a, total suspended sediment, visibility, and CDOM) and hydrodynamic data (water level, currents, temperature, and salinity) generated from the hydrodynamic model. CNN-II with 300 times large dataset (7x7 segmented image) showed better prediction accuracy with R^2 exceeding 0.91 and low average RMSE (0.191). Also, the model predicted that CDOM plays a vital role in estimating the spatial-temporal distribution of Chl-a from the satellite colour data. Likewise, a neural network model named Ocean Colour Net (OCN)) with match-up datasets showed to improve the Chl-a estimation on the surface and within the productive zone of the Barents Sea using satellite imagery data (Asim et al., 2021). A new spatial window-based match-up dataset was created by matching depth-integrated *in situ* Chl-a concentration with the multispectral remote sensing images from Sentinel-2. After removing the erroneous samples in the match-ups datasets based on satellite reflectance, the OCN was trained and tested with the match-ups dataset. OCN outperform the existing ML models (Gaussian Process Regression (GPR), Ocean Colour (OC3) algorithm, Case-2 Regional/Coast Colour (C2RCC) and the spectral band ratios) with less mean absolute error. Also, the spatial window and depth-integrated match-up dataset improved the performance of the OCN by 57%.

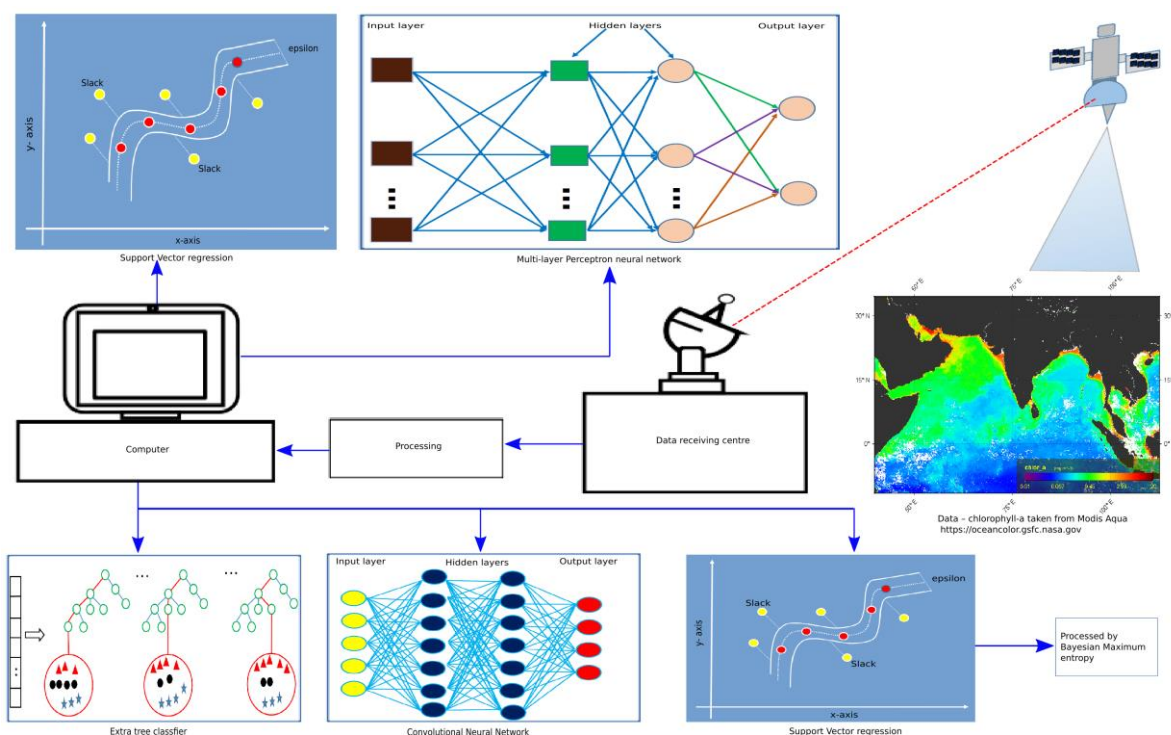


Figure 2. Use of ML algorithms to measure and estimate the ocean surface chlorophyll-a from satellite data.

3.1.3. Numerical dataset-based plankton classification.

ML algorithms like M5P and regression trees integrated with the WEKA were used to study phytoplankton dynamics in station RV001 in front of Rovinj, open Northern Adriatic Sea (NAS) (Volf et al., 2014). The first model (M5P) identifies the factors that influence the phytoplankton abundance in the NAS from the 28 years (1979-2007) dataset containing phytoplankton concentration along with the physicochemical parameters (salinity, temperature, river flow (Po River), month, year). M5P model predicted salinity and temperature as essential factors that influence the phytoplankton abundance, and a significant change in phytoplankton dynamics occurred at the NAS in 1998 and three years (1985, 1989, and 1993) before 1998 (coefficient correlation of 0.7). Where the second model successfully forecasts the phytoplankton concentration with a good coefficient correlation of 0.82. This type of model may help understand the functional ecosystem. However, a consensus model (Weighted Average Prediction Error (WA-PE) model) created by combining four single-model predictions (SVM, RF, Boosting and generalised linear models) successfully predicted phytoplankton species with low classification error from the phytoplankton (eight) presence and absence data (Bourel et al., 2017). The model WA-PE showed low classification error in classifying *Akashiwo sanguinea* and *Dinophysis acuminata* (10% and 38%, respectively).

Apart from the environmental variables influencing the phytoplankton variability in the time-series study, the uncertainty caused in the laboratory was also predicted by two ML algorithms (Bray Curtis distance and pairwise permutational multivariate analysis of variance) (Muñiz et al., 2020). Bray Curtis distance showed that the long time-series phytoplankton variability studies significantly influenced different experts handling the sample and fixatives used. Also, PERMANOVA showed significant variations between dyes used (glutaraldehyde and Lugol's solution) and between the taxonomists involved in the study.

Genetic programming (GP) efficiently identified the strong association between a rise in water temperature with reduced Net Primary Productivity (NPP) in the oligotrophic ocean (D'Alelio et al., 2020). The 27 years Bermuda Atlantic Time-series Study (BATS) dataset contains NPP and environmental parameters. GP showed reduced NPP due to warming and weakening of vertical mixing in the upper water column, which reduces the nutrient availability (light and nitrogen). This model indicates the necessity to have a long-term monitoring study with advanced omics techniques in the oligotrophic region of the ocean to understand the early trends better and predict future oceanic conditions. A neural-network-derived quantitative niche model predicted Pico-phytoplankton lineages separated into latitudinal niches based on the cell size and showed increased biomass along the temperature gradient in low-latitude regions (Flombaum et al., 2020). The model also predicted (based on the global dataset) a high concentration of cells found in the North Atlantic (above 45°N), around the North Pacific Current, and a band near the southern subtropical convergence zone. In comparison, oligotrophic gyres and polar regions showed a low concentration of cells. The model also predicts future increases in seawater temperature in low-latitude regions may lead to an increase in the biomass of picophytoplankton, which is also supported by the elevated upper-ocean nutrient recycling and lower nutrient requirements of phytoplanktons.

3.1.4. Harmful Algal Bloom (HAB)

HAB is the rapid proliferation of microscopic algae or phytoplankton (including blue-green algae) and accumulates toxic or other noxious substances. Some HAB produce non-toxic compounds that react with reactive oxygen species, polyunsaturated fatty acids, and mucilage. These HAB are lethal to fishes and cause faunal mortality via high biomass accumulation, leading to oxygen depletion (Anderson et al., 2012). HAB causes fish deaths worldwide, and these issues appear to be frequently growing. Developing early-warning systems is one approach to reducing their effects on people's health and livelihoods (Yñiguez & Ottong, 2020). Fisher's linear discriminant analysis (LDA) classified algal blooms based on spectral properties at the order level. The spectral properties of 53 different unialgal cultures were used as training data. LDA spectral properties with

a leave-one-out cross-validation method and cross-examined with mixed algal culture LDA excellently classified cyanobacteria from other algal groups, with an accuracy of 81.5% and 100% algal group. Also, LDA had a low error rate of 9.3% or no error rate in identifying dinoflagellates and cyanobacteria, respectively. LDA had 96.3% accuracy in identifying dinoflagellates, cyanobacteria, and other algal groups. Likewise, Yñiguez & Ottong (2020) developed two early warning systems to detect harmful algal bloom using RF.

A two-year field sensor dataset of temperature, salinity, dissolved oxygen, pH and chlorophyll, and shellfish ban, and fish kill occurrences from Bolinao-Anda, the Philippines, were used to train the RF model. RF model had an accuracy of 96.1% for the fish kill with dissolved oxygen, higher temperature, and salinity as essential factors. The model had 97.8% accuracy detecting shellfish ban, influenced by low salinity and higher Chl conditions. These models might have applications in the real-time monitoring of HABs in marine environments.

3.2. Zooplankton classification

Zooplankton (ZP) are highly abundant and plays an important role in the ocean's biogeochemical cycle. These ZP are highly diverse and range from microzooplankton to metazoans. Classification of ZP through image is much more challenging than the phytoplankton, as ZP have different sizes and morphology. Even though they have distinguishable differences between the groups like copepods and euphausiids, they possess remarkable similarities between the closely related genera (e.g., *Calanus* spp. and *Paracalanus* spp.), which makes the identification of ZP highly challenging. Also, manual identification requires a skilled taxonomist and is a time-consuming process. So automatic identification through images is an alternate methodology. The identification and measuring of the size of ZP through images started in the 1980s, from Silhouette imaging (Jeffries *et al.*, 1980) and images (Rolke and Lenz, 1984). Early ML algorithms like discriminant analysis were used to identify the frequently observed eight ZP taxonomic groups from images (from the coastal waters of England, which had an accuracy of 89%) (Jeffries *et al.*, 1984) and flow-through sampler images (Berman, 1990). All the above methods have disadvantages like the image quality (orientation of objects and low contrast) and small dataset.

NN algorithms such as a backward error-propagation neural network identified ZP with a reasonably small dataset (Simpson *et al.*, 1991; Culverhouse *et al.*, 1994), and Learning Vector Quantization classifier (LVQ) with Fourier feature classified the images captured by the Video Plankton Recorder (VPR) (Tang *et al.*, 1998). Also, a combination of different neural networks was used for pattern recognition (Tang, 1998). LVQ with extracted ROIs and different neuron numbers

measured the size and abundance of ZP from large image datasets (Davis et al., 2004). Even with the neural networks, the accuracy was less while detecting relatively low abundant ZP, which was considerably improved (50% relatively low abundant taxa) by the SVM classifier with the co-occurrence matrices as a feature. Also, the model showed a reduced error rate (Hu and Davis, 2005). Similarly, a new discriminant vector forest algorithm which is a combination of LDA, LVQ and RF, identified 2000 items per second at an accuracy of 75% from the ZooScan images (Grosjean et al., 2004), ZooScan captures ZP images with a 2400-dpi resolution, and the model was chosen based on the validation (Grosjean et al., 2004). Along with SVM, decision trees and other unsupervised algorithms are also used to identify ZP, which have 70 - 80% accuracy (Irigoien et al., 2006).

Although these methods showed considerable accuracy, they have some disadvantages that required manual sorting of images, trained only with lab-preserved samples, poor image quality and slow computation power. To overcome this, a fully automatic dual classification system was utilized (Hu and Davis, 2006) where the planktons were identified by an LVQ using shapes as features followed by SVM using texture-based features. In 2007 ZooImage was created to predict the taxonomy of preserved ZP (Grosjean & Denis, 2007), which had an accuracy of 70 – 80% in identifying 10 - 20 taxonomic groups of ZP (Benfield et al., 2007). This ZooImage (automated system) with RF showed difficulties in classifying field samples, where the accuracy dropped to 63.3% from 81.7% when the other non-living substance was removed from the samples. Also, the model predicted ZP size as an essential feature in classification (Bell & Hopcroft, 2008). Later the combination of ZooScan, Zooprocess and Plankton Identifier software (PkID) with RF (to identify) and manual validation identified ZP with better accuracy. RF was chosen based on the performance compared with six other classifiers. The PkID had a better performance with RF and classified ZP moderately with 80% accuracy from the Villefranche time-series datasets (Validation), and the performance was slightly improved after manual validation (Gorsky et al., 2010).

All these models predict only the highly abundant taxa, Estimation of low abundant rare taxa diversity and composition is still challenging. A semi-automatic model with a naïve Bayesian classifier (NBC) overcomes these difficulties. With manual validation, NBC predicted rare taxa at high accuracy, which helps estimate diversity indices (Ye et al., 2011). Moreover, with simple geometric features, the combined GBC and SVM model had better performance with 88.6 % accuracy in classifying eight classes of ZP (with 4000 and 1000 training and testing images, respectively) (Ellen et al., 2015). Also, ML algorithms solved the ecological conclusions (distribution patterns), and the dataset of post-processed Zooprocess and PkID with RF showed that

the distribution predicted by the model was similar to the reference distribution. With the RF model defined probability score, the accuracy was increased by 16% after removing the class with a probability threshold of 1% error rate (84% accuracy). Most importantly, the model automatically predicted the difference in the distribution of abundance over a larger region and pattern between day and night (Faillettaz et al., 2016).

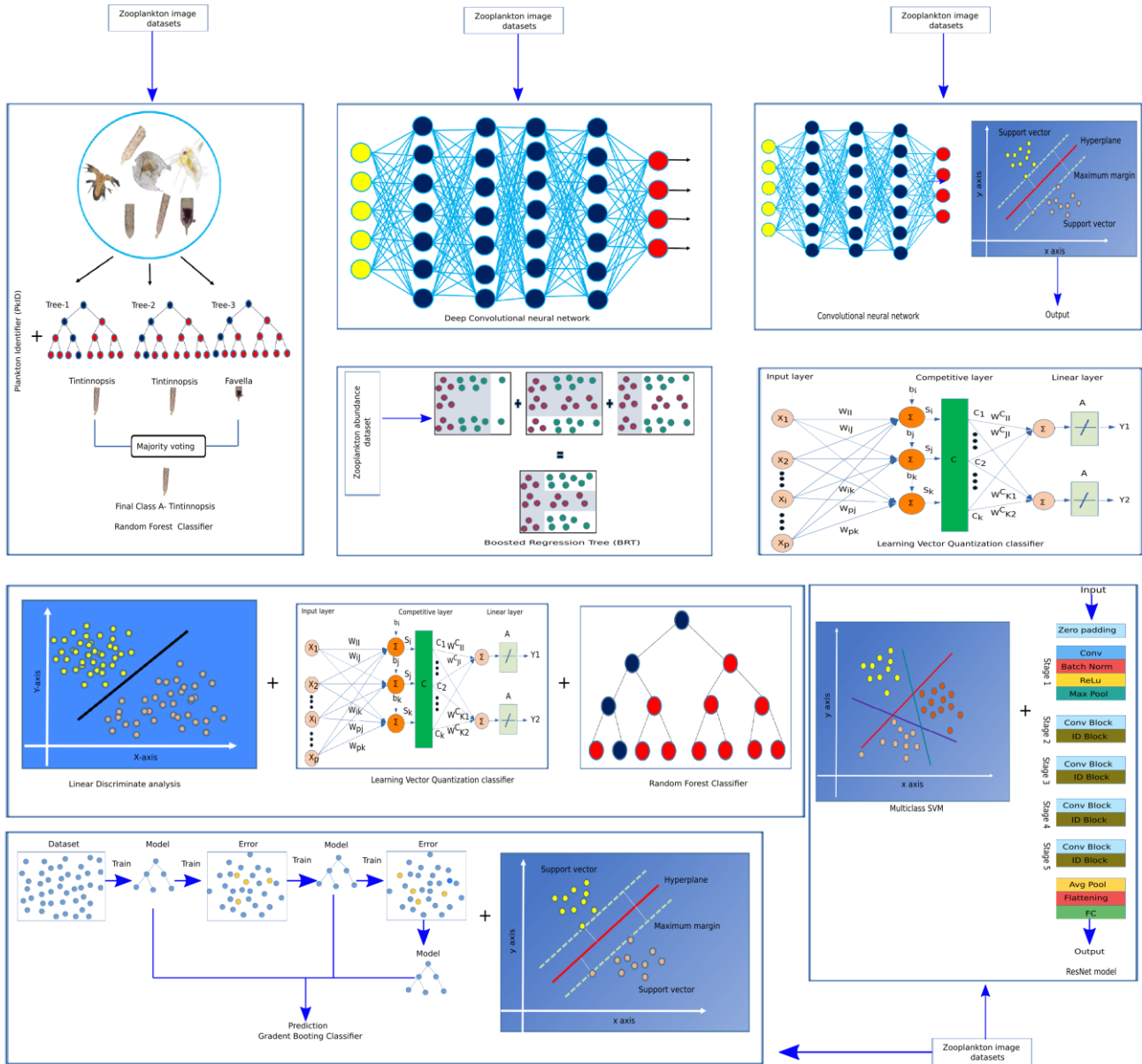


Figure 3. ML algorithms are used to identify or classify zooplankton through images captured by various underwater devices.

Earlier, deep learning methods were used to detect and classify ZP, but a large dataset is required for Deep Learning, CNN and ensemble models. The ZP image dataset was relatively small compared to previous studies and consisted of a class imbalance problem (lack of images for low

abundant ZP). Where the low abundant taxa were not predicted by most of the ML algorithms, these problems were addressed using a deep learning architecture, "Zooplankton", an automatic classifier which reduces the overfitting caused by lack of data by applying data augmentation. Using general and representative features rather than pre-defined extraction algorithms, CNN classified ZP with 93.7% accuracy (Dai et al., 2016). Also, a deep residual network classifies plankton from images with an accuracy of 95.8% (at 9.1 fps) (Li and Cui, 2016). Later, CNN (a spatially sparse) identified ZP with an accuracy of 84% (recall rate of 40%) from 2.4 million images captured by the advanced imaging system *In Situ* Ichthyoplankton Imaging System (ISIIS). CNN identified 108 plankton from a forty-hour underwater image data collected from the eight transects in the northern Gulf of Mexico. Also, the accuracy was increased to >90% when rare taxa were removed (Luo et al. (2018). Similarly, the YOLO v2 model performed considerably well (with a precision of 94% and a recall rate of 88%) in classifying ZP from the holographic images with a sharpness assessment score equal to 0.6 or more (Shi e et al., 2019). This approach demonstrated that the efficacy of CNN would be applied to various plankton and biological imaging classification systems with eventual application in ecological and fisheries management. In combination with SVM with different CNN, models showed increased classification and recalled accuracy (7.13% and 6.41%, respectively). Where CNN extracted the ROIs (from the plankton images), the ROIs were enhanced by removing background noises. Among the CNN, ResNet50 with multiclass SVM showed the best accuracy and recall (94.52% and 94.13%, respectively) (Cheng et al., 2019).

However, CNN had difficulties identifying ZP when the images were rotated at a certain angle. This rotational variance was overcome by the combined model (CNN and SVM) which had a mechanism that mimicked human eye movement to extract features (Cartesian coordinates and polar coordinates). Then these vectors were fused and used to train the convolutional learning, later classified by SVM. The model had high accuracy (94.91%) and recall rate (94.76%) (validated) against the CIFAR-10 image dataset (Cheng et al., 2020). Moreover, a sparse CNN identified 64 ZP taxa from the ISIIS collected on the Oregon coast, USA, with an accuracy and recall rate of 83% and 56%, respectively (Briseño-Avena et al., 2020).

The main idea behind the ML algorithms is to apply them in the field and to measure in real time. A novel mobile robotic tool, "AILARON" (Automatic Underwater Vehicle), was created to characterise the upper water column biota. The images captured by the silhouette camera were classified by deep learning and grouped based on the probability score. This processing pipeline consists of imaging, supervised machine learning, hydrodynamics, and AI planning, which process each image in an average of 3.852 seconds. AILARON may be useful to enhance the knowledge of

plankton communities and their Spatiotemporal distribution patterns and have great importance in ecosystem surveillance and monitoring global change (Aya Saad et al., 2020).

Apart from the identification and Estimation of ZP, ML algorithms were used to predict the changes in ZP abundance and occurrence based on the environmental conditions. Boosted Regression Tree (BRT) model predicted the space and time measurements of six zooplankton abundance in SO (Copepods, Foraminifera, *Fritillaria* spp., *Oithona similis* and Pteropods). Based on the abundance and environmental datasets the model predicted that over two decades (1997 to 2018) the environmental conditions changed in favour of copepods, Foraminifera, and *Fritillaria* spp. (increased the abundance by 0.72% per year). Also, the conditions in the Ross Sea shelf regions have significantly deteriorated the pteropods' abundance (Pinkerton et al., 2020). Moreover, RF with manual correction of ZooImage successfully classified all copepods classes with precision and recall ranging between 0.07% – 0.20% and 0.82% – 0.94%, respectively. Based on the RF and manual correction, 25% of the total annual abundance in the Mediterranean Sea was recorded in April alone, and the lowest of ZP abundance observed in spring was influenced by wind gusts, nitrate availability and water temperature, which is in sync with increase in seawater temperature in winter (Fullgrabe et al., 2020).

The detection and classification of ZP can be approached viz., high quantity of features and optimisation of classification models to prevent feature loss. The detection of rare ZP taxa through deep learning has some limitations. One such limitation is the class imbalance and reduction of plankton's feature loss in neural networks. Eight different rare ZP were identified using NBC (using posterior probability and predictive confidence value), with accuracy ranging between 0.18 to 0.87 (Ye et al., 2011). Many studies used data augmentation to create training datasets by capturing images in different brightness, image orientation angle, etc. (Dai et al., 2016; Cheng et al., 2020; Shi et al., 2019). One such data augmentation technique is the use of Cycle-consistent Adversarial Network (CycleGAN). The data generated by CycleGAN was successfully classified by a densely connected YOLO V3, which outperformed previous state-of-the-art models with mean Average Precision (mAP) of 97.21% and 97.14% (two experimental datasets with varied numbers of rare taxa). The model also improved the accuracy of detecting rare taxa by an average of 4.02% and has the potential to be included in autonomous underwater vehicles for real-time identification and plankton ecosystem observation (Li et al., 2021). The model proposed by Gorsky et al. (2010) - ZooScan and ZooProcess was successfully implemented in the identification and estimation of ZP abundance in the bay of Villefranche-sur-Mer, France (Feuilloley et al., 2022). This shows that ML algorithms are a potential tool not only for the identification of ZP but also used to solve ecological

problems. Still, few improvements are required in this field to achieve full automation to detect rare taxa and morphologically similar species.

3.3. Identification and classification of fishes and mammals using acoustic data

Most marine mammals and fishes produce acoustic (sounds) to communicate within the group or species or to locate prey. This acoustic has different frequency range, and the frequency differs based on the animal that produce. As an alternate method to visual identification, these acoustic data were used to study the animals' behaviour. Automatic analysis of acoustic data and identification of individual clicks produced by individual marine mammals are challenging. The acoustic signals are influenced by many factors like the depth in which the animal dwell, orientation and the distance from the hydrophone (Thode et al., 2002; Møhl et al., 2003). Few studies used wavelet transformation (mathematical models) to analyse clicks (Adam et al., 2005; Lopatka et al., 2005; van der Schaar et al., 2007). This method faced difficulties in characterising dive clicks. The use of ML in the identification of animals from their acoustic data started in the early 90s. A back-propagation neural network (ANN) accurately discriminates acoustic from the individual orca, as well as the same calls from other whales within the group (Gaetz et al. 1993). It also discriminates the *Orcinus orca* behaviour based on the acoustic data. This approach not only enhances knowledge of whale behaviour based on acoustic calls without the need for visual confirmation but also reduces the time that inexperienced observers take to identify the whales.

Similarly, Bienstock, Cooper and Munro (BCM) unsupervised neural network successfully classified different mammal sounds, even those recorded from different geographical regions (Huynh et al., 1998). Likewise, the unsupervised ML-NN (a self-organising network) detect and categorise the vocalisation of false killer whales without any pre-defined categories (Murray et al., 1998). The 2D dataset contains short measures of duty calls, and the peak frequency of false killer whale vocalisations was analysed using two-NN, where the competitive learning (first neural network) recognises vectors that are frequently presented in input vocalisation and categorise them in class patterns. The Kohonen feature map (second network) provides patterns relationships (graphical representation) for the outputs defined by the first NN. The model performed well in categorising vocalisation and the ability to classify the vocalisation of other mammals. Also, a radial basis function network model (a two-layer neural network) successfully separated the individual whales' clicks from a group of hunting sperm whales' recordings (Van der Schaar et al., 2007). The NN trained with six individual male diving clicks, consisting of five short and one complete diving click. A wave-based local discriminant basis extracted the features (clicks), and the extracted features were used to train the model with 50 clicks from each dataset and the rest of the

clicks were used for testing. The model classified the short and diving clicks with 90% and 78% accuracy, respectively.

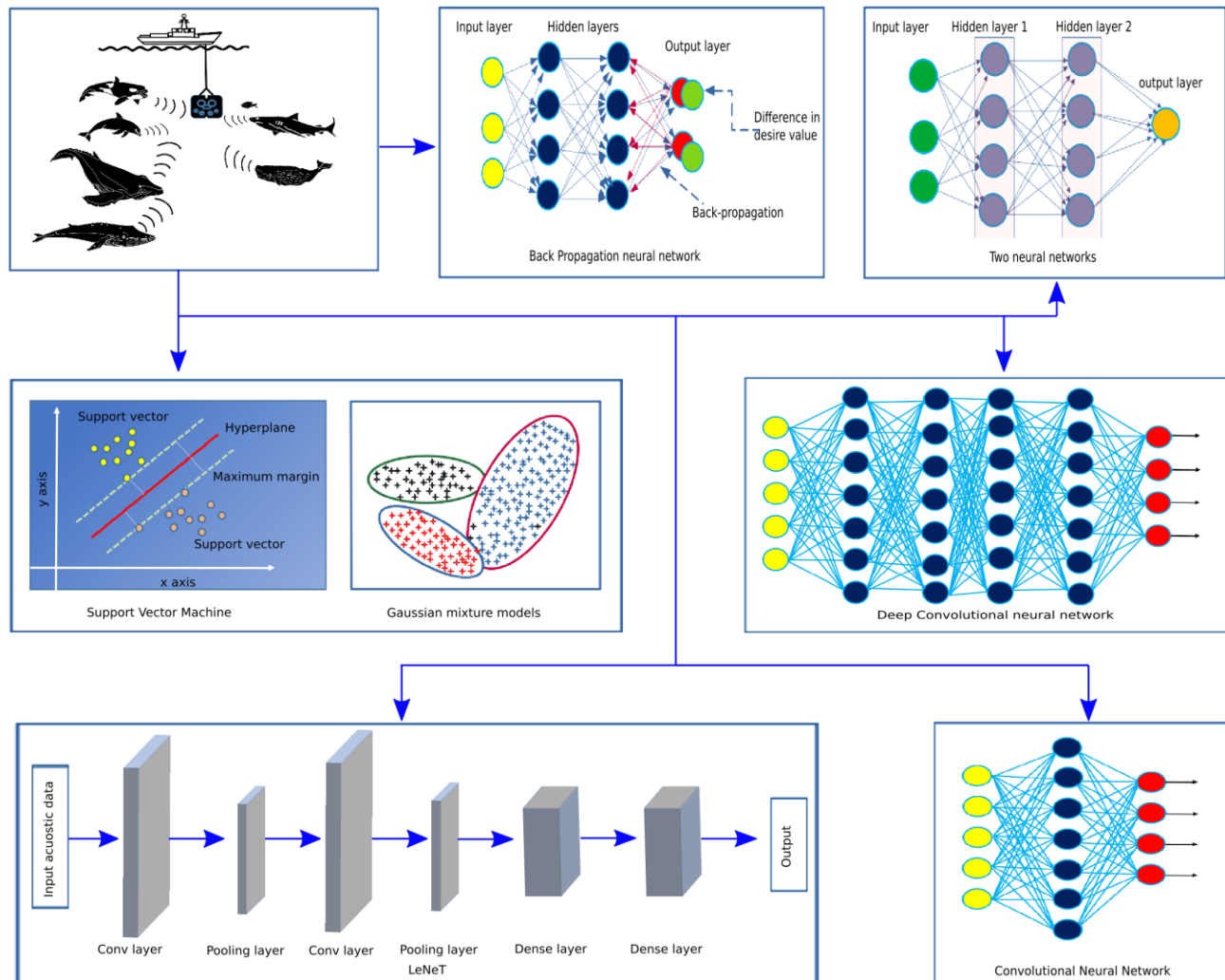


Figure 4. ML algorithms are used to identify and understand the behaviour of marine fishes and mammals from acoustic data.

Similarly, the bioacoustics behaviour of *Physeter macrocephalus* (sperm whale) was effectively classified using CNN based click detector (Bermant et al., (2019)). Based on the presence and absence of clicks in the spectrogram, CNN successfully classified 650 spectrograms with an accuracy of 99.5%. Furthermore, a trained CNN-based click detector successfully classified three types of tasks, i.e., coda type classification, vocal clan, and classification of individual whales using Long-term memory and gated recurrent unit recurrent neural networks. The CNN showed high accuracy in classifying 23 and 43 coda types from the Dominica dataset (with an accuracy of 97.5%) and the Eastern Tropical Pacific (ETP) dataset (with an accuracy of 93.6%), respectively. Also, the model has an accuracy of 95.3% for the Dominica dataset (for two clans) and 93.1% for

the ETP dataset (for four types of clans) in classifying the vocal clan. Moreover, the model has 99.4% accuracy in identifying individual whales' clicks. These results demonstrate the feasibility of applying CNN to classify sperm whale bioacoustics and learning fine details of whale vocalisations. In advance, deep neural networks successfully detect the vocalisations of the endangered North Atlantic right whale *Eubalaena glacialis* (Shiu et al., 2020). Different deep learning models were tested where the LeNet performed better with the lowest false positive rate. Three datasets from the Detection Classification, Localisation, and Density Estimation of Marine Mammals (DCLDE 2013) dataset, MARU deployments dataset and kegg (whale competition-Massachusetts) were used for the study. LeNet not only had significant high precision and recall than the algorithms presented at the DCLDE 2013, but CNN trained with recordings from one geographic location over a period of time, was able to recognise calls spanning many years and across the species' range with a low percentage of false-positive rate. It is also simple to integrate into current software, allowing researchers to learn more about endangered species.

ML algorithms other than neural networks were used to study acoustic data. The clicks produced by either one or more individuals of the following species, i.e., Blainville's beaked whales, short-finned pilot whales, and Risso's dolphins, were differentiated by Gaussian mixture models (GMMs) and SVM (Roch et al., 2008). The Teager energy operator locates the individual click from the echolocation clicks recorder, and cepstral analysis constructs the feature vectors for these clicks. Two detectors based on GMMs and SVM trained with the cepstral feature conform or reject the species based on the clicks, GMMs model the time series of independent characters of species feature distribution and SVM model the boundaries between the species feature distribution from one species to another. Both models detect the clicks with less error rate.

The sensitivity level between the different abiotic variables and acoustic density of fishery resources (two different layers) in the Northern South China Sea was estimated using Extreme Gradient Boosting (XGBoost) and RF (Sun et al., 2020). The fish density acoustic data from the surface mixed layer and bottom cold-water layer, along with the abiotic variables (temperature, salinity, water depth, nitrite, nitrate, ammonia, and phosphate), were used to train and test ML models. The acoustic data were characterised by Nautical Area Scattering Coefficient values (NASC). XGBoost predicted the surface temperature, and nitrate had a high sensitivity value with the NASC value at the surface mixed layer (10 m), whereas RF predicted the surface temperature as a significant factor for surface NASC value. In the bottom NASC, the nitrate at 10 m and the surface temperature had a high sensitivity score (Xboost), whereas RF predicted the surface

temperature, nitrate concentration at 0 m and temperature difference between the surface and bottom layers as essential factors for bottom NASC.

ML algorithms are used not only to identify the clicks generated by the mammals but also to understand the animals' behaviour based on the accelerometer. The five different behaviours (chafing, burst swimming, head shaking, resting, and swimming in a semi-captive setting) of young lemon sharks (*Negaprion brevirostris*) were characterised by a voting ensemble (VE) model (Brewster et al., 2018). In addition, the model predicts the time of day, tidal phase, and season, which are all important aspects in determining lemon shark feeding and provide insights into their feeding ecology. Deep learning was also used to identify the alien species based on the sound they produced (Demertzis *et al.*, 2017 and 2018). Spiking Convolutional Neural Network (SCNN) effectively generalises the sound produced by different animals (Sea Audio Dataset). SCNN recognise mammals' sound with high accuracy and recall, whereas the recognition of fishes was a little tricky (Demertzis *et al.*, 2017). With online learning algorithms, a new Online Sequential Multilayer Graph Regularised Extreme Learning Machine Autoencoder (MIGRATE_ELM), which has an innovative Deep Learning algorithm (DELE), was trained with the Sea Audio dataset and showed slightly high performance than SCNN. In many cases, this algorithm produces equal and slightly high accuracy than the previous SCNN model. However, it reduces the implementation time by 23% more than the SCNN.

3.4. Image-based identification and classification of marine macro-organisms

Similar to classification and behaviour characterisation using acoustic datasets, ML algorithms were also used to classify and identify fishes, mammals and other marine animals from the underwater images. Classification and identification of marine animals through images also help monitor animals' health conditions and environment. Recent developments in underwater imaging technology created a massive volume of data, making manual identification a time-consuming and challenging process. Also, the complexity of underwater circumstances such as light, temperature, suspended particles and pressure influence identification. Using an automated analyser supported by ML algorithms is an alternate option.

The real-time detection of fish or animals is a difficult task because of the complexity of underwater video or image datasets. Few studies used ML algorithms to detect underwater fishes and other animals. The Sparse Representation-based Classification (SRC-MP) with Eigenfaces and Fisherface (extract features from images) recognises the fishes in the coral reef ecosystem of southern Taiwan (Hsiao et al., 2014). Best recognition and identification rates were observed when SRC-MP with

Eigenfaces (81.8% and 96%, respectively). Similarly, the fish from the underwater videos (using Fish Recognition Ground-Truth dataset-FRGT) were successfully identified by the linear SVM classifier (accuracy 98.64%) with Spatial Pyramid Pooling (SPP) for features extracted (Qin et al., 2015). However, these models use one or various features, and improving the accuracy requires large datasets. The problem of inadequate data was solved by implementing transfer learning and deep learning models (Tamou et al., 2018; Liu et al., 2019). The linear SVM classifies the fish with features extracted by the pre-trained AlexNet (Tamou et al., 2018). The FRGT dataset AlexNet and linear SVM classifier classify the fishes with 99.45% accuracy.

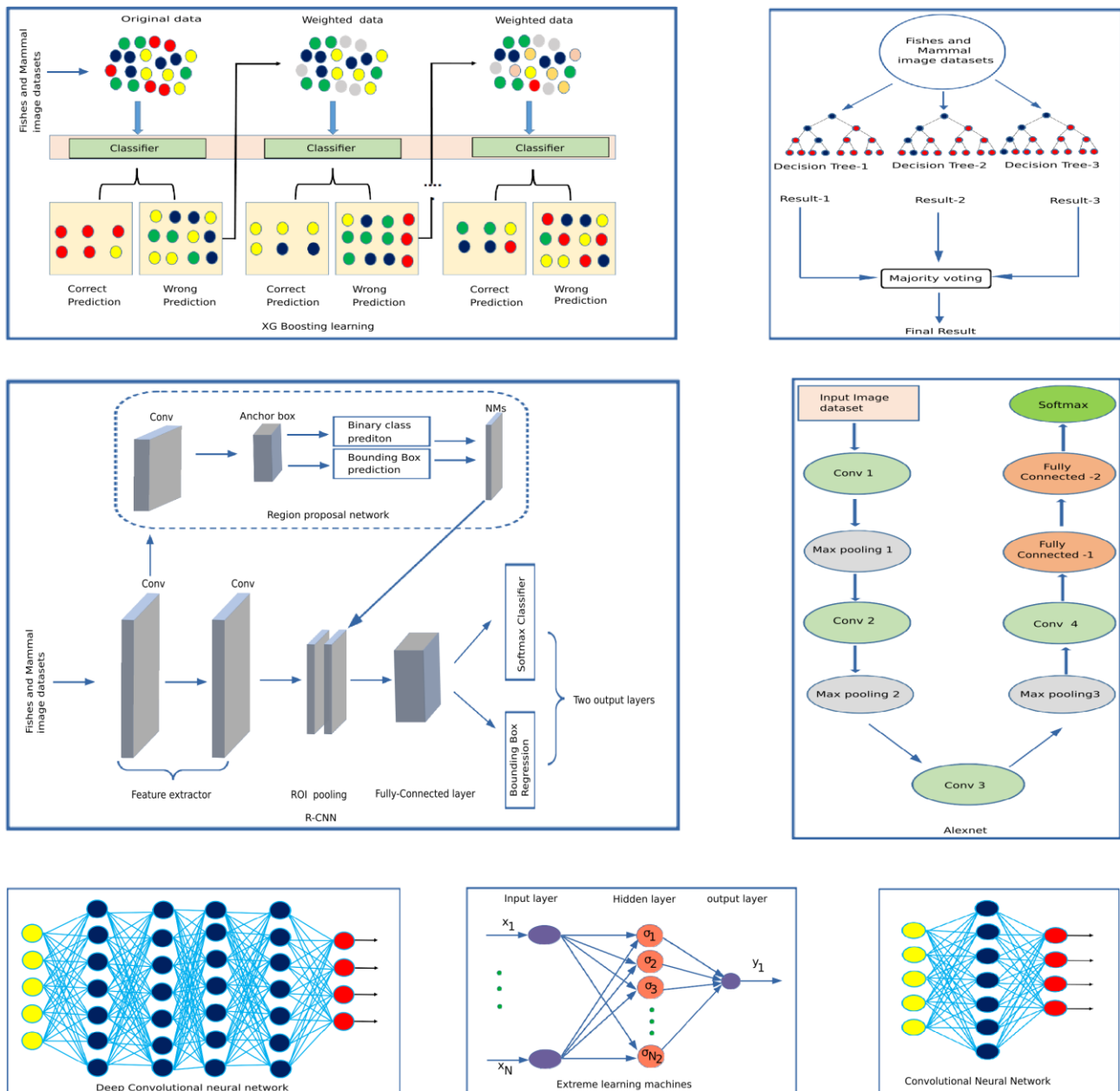


Figure 5. ML algorithms are used to identify and classify marine organisms from image datasets.

Similarly, the transfer learning applied to the MobileNet v2 model had high validation accuracy (92.89%) and less computing time than Inception v3 and MobileNet v1 in identifying fishes. Also, the model was 40M in size, which is suitable for embedding in a device for real-time classification of marine animals from the underwater image. To overcome the limitation of datasets, Allken et al. (2019) created a unique training dataset synthetical (realistic simulation of Deep Vision) from images captured from the camera fitted to the trawler system. This dataset was used to train the deep neural network, which successfully identifies blue whiting, Atlantic herring, and Atlantic mackerel with an accuracy of 94%. This method of creating synthetic data from the collected data may successfully overcome the shortage of training data.

Also, the difficulties in identifying fish from the blurry ocean images and the lack of training sets were overcome by a CNN model using data augmentation, network simplification, and speeding up the training process. In this model, overfitting was solved by the dropout algorithm, and the loss functions were refined to update the parameters inside the network (Cui et al., 2020). These processes speed up the training process and reduce the training loss. Also, the model shows good accuracy and is suitable for embedded systems with the autonomous underwater vehicle. The combination of human annotation with ML algorithms successfully handled large underwater image datasets to classify mesofauna (Langenkämper et al., (2019). Two-step human annotation followed by ML classification was used. The datasets were first annotated by humans and classified by AlexNet. The model shows the inaccuracy in human annotation as a significant factor that affects classification accuracy, where the marking size and false positives show a minor influence. Even with advanced deep learning algorithms, the rate of misclassification is high. To reduce the misclassification rate was reduced by introducing a species-specific confidence threshold. A CNN-based framework automatically calculates species-specific confidence threshold value from the training dataset (Independent of the data used to train the deep learning algorithm). These threshold values are used in the post-processing of profound learning outputs, assigning classification scores for each class and marking a new class as unsure from the images (Villon et al., 2020). Applying species-specific threshold values reduces the misclassification rate from 22% to 2.98% in identifying 20 fish species from 13,232 images from coral reef environments.

Besides fish identification, ML algorithms were also used to identify and count whales. The CNN (two-step) successfully identified and counted whales from the image data sources such as satellite and aerial pictures (Guirado et al. (2019). The first CNN detected the presence of whales in the images, and the second CNN counted the number of whales in those images. The model showed 81% and 94% accuracy in detecting and counting whales from 10 global whale-watching hotspots

(Google Earth images datasets) and combining these two CNN increased the detection rate to 36%. This new tool improves the ongoing efforts in mammal watching and conservation from the vast uncharted regions of the sea. Increasing the availability of satellite and image datasets will lead to better monitoring endangered mammals.

Exploring deep sea animals by humans is challenging, because of the hostile conditions, so identification through images or videos with the aid of ML algorithms is more suitable. However, the identification of animals from the images has difficulties, as the underwater images have uneven lamination, noise, and low contrast, which required some improvements. A modified deep CNN based on Region based-CNN (R-CNN) and a modified hypernet method successfully detect and classify underwater marine organisms (Han et al., 2020). Datasets from a remotely operated vehicle (ROV) (video from a sea cucumber fishing site) and an underwater robot picking contest were used, and the Regional Proposed Network optimised the feature extraction. The CNN model performed well in recalling and detecting organisms, even with a different focus. When the Intersection over Union equals 0.7, the mAP was more than 90%. The model seems suitable for analysing organisms' real-time detection from a camera installed in an ROV.

Similarly, the problem in the deep-sea underwater images, like uneven lamination, noise and low contrast, was successfully overcome by image enhancement using a combination of two methods, max-RGB and shades of grey. In comparison, weak illumination was solved by CNN. After pre-processing, scheme two detects and classifies the animals at 50 frames per second detection speed with a mAP of 90%. This ML algorithm is helpful in real-time detecting underwater organisms and can assist underwater robots in avoiding dangerous high-pressure conditions and helping humans understand deep-sea environmental conditions.

A deep neural network along with Marine Object-Based Image Analysis (MOBIA) efficiently identified the individual organismal distribution and zonation across the CWC Piddington coral mound in Ireland (Conti et al., 2019). 2 mm high-resolution reef-scale video mosaic and multibeam data from ROV from the CWC Piddington coral mound within the Porcupine Seabight, Ireland Margin were used for the training. Among the tested models (decision tree, logistic regression, and deep neural network), the deep neural network had higher classification accuracy and recall, which showed that the mound was made up of 12.5% coral rubble, 2% of live corals and 3.5% of heterogeneous distribution of sponges in some parts of the mounds. Applying ML provides a baseline to monitor the changes in the mounds. This method can be applied to other habitats to monitor the modifications over a period of time. Likewise, the coral species in the shallow water of

the Gulf of Eilat were identified from the underwater images using CNN (Raphael et al., 2020). The CNN successfully overcome the difficulties like coral colony, age, species, species morphology, depth, water current, quality of image, angle of view etc. With a dataset consisting of 11 well-known coral species (Five thousand underwater images), the model showed an overall accuracy of 80.13% for all 11 species of corals. Among the 11 species, the CNN had high accuracy ranging between 91.5% to 93.5% in identifying *Montipora*, *Lobophyllia* and *Stylophora*. Future deep learning might be used for real-time monitoring of the effects caused by global climate change on corals in Eilat and other corals around the world. In addition to these studies, a large-scale dataset, "DeepFish", was created using ResNet-50 (Saleh et al., 2020). DeepFish contains images of fishes from the underwater marine environment in tropical Australia (20 different marine environments), and this dataset is available and suitable for training and testing different ML algorithms.

3.5. Identification and classification of benthic fauna

Megafaunas play an essential role in the functioning of the benthic ecosystem and act as indicators of environmental change. Manual species identification is time-consuming, and most ecological studies frequently neglect this organism size class. Automated image analysis is a possible way to address the practical challenges in identifying mesofaunas. However, the diverse megafauna populations make such automated approaches difficult. Schoening et al. (2012) created an automatic image analysis system called intelligent Screening of underwater Image Sequences (iSIS) to quantify and examine the diverse group of megafauna species. The iSIS had three steps, i.e., feature extraction, training SVM with extracted features and utilising human labelled images containing mesofauna taxa. Then the model predicts the possible taxa position and counts the number of taxa in every field of view. The iSIS performed similarly to human experts when the seabed image dataset was used (consisting of eight distinct species recorded in the Arctic deep-sea observatory (HAUSGARTEN)). Taxa like *Bathycrinus stalks* and *Kolga hyalina* were well identified by iSIS. Some species of *Elpidia heckeri* (little sea cucumber) remain difficult for both iSIS and human experts. As a result, advancements in computer-assisted benthic ecosystem monitoring might be an alternate method for reducing human time and limitations.

Likewise, the benthic biodiversity was identified by the inception v3 model (TensorFlow) from the underwater images. The model was trained with increasing images (20 to 1000 images per taxa) and taxa (7 to 25). The model performed best when two hundred images per taxa (0.78 sensitivity, 0.75 precision) and the least number of taxa were used. Even though the model was not an alternative to manual annotation, this technique classified individual taxa from the images with high precision.

This model might help non-experts study benthic diversity, which leads to an increase in the database for conservation (Piechaud et al., 2019). Also, identifying broad-scale patterns in the benthic faunas is too difficult because the individual benthic surveys could not compare directly. The reliable comparison typically depended on a common set of habitats or a one-off broad-scale spatial survey. Cooper & Barry (2020) match the new benthic fauna survey data with the existing broad-scale cluster group using unsupervised K-mean algorithms. This example provides a way to compare individual surveys to identify the macrofaunal clustering patterns. Also, this approach improved the understanding of benthic faunal distribution patterns. Cooper & Barry (2020) also created a R shiny web application that allows investigators to match habitat with their collected data.

3.6. Microbiology

Several researchers have applied ML algorithms to identify or solve the microbes-related problem in the marine system. We have listed a few studies that use ML's potential to solve problems in marine microbiology. High throughput metagenome sequencing was used to identify the microbial diversity in different environments from hypersaline sediment (Sadaiappan et al., 2019) to SO waters (Sadaiappan et al., 2022). Likewise, RF was used to successfully characterise sponges into high microbial abundance (HMA) and low microbial abundance (LMA) groups based on the phylum and class dataset. RF model understands the patterns of the host-associated microbiome and, based on the Operational Taxonomic Units (OTUs), predicted the status of 135 sponge species without prior knowledge and divides sponges into four groups (top two groups consist of HMA = 44 and LMA = 74, respectively). RF proved a valuable tool for addressing host-associated microbial communities' biological questions (Moitinho-silva et al., 2017). Likewise, ML algorithms were successfully applied to differentiate ballast water from the harbour and open sea waters by using 16S rRNA gene sequencing data. Based on the 16S rDNA OTUs, LefSe, LDA, and RF predicted sample-specific biomarkers (8 bacteria), which were used in other classification models. With these biomarkers, KNN accurately (80%) differentiated the ballast water samples from the harbour and open sea waters samples (Gerhard & Gunsch, 2019). Moreover, a strong link between the genome content and ecological niches was predicted by the Gradient boosting (GB) model. About 1961 metagenome-assembled genomes (MAG) were binned from 123 water samples in the Baltic Sea, which belong to 352 species-level clusters corresponding to 1/3 of the metagenome sequences of the prokaryotic size fraction were used in the prediction. ML proved that other than phylogenetic signals, gene contents can be used to predict ecological niches (Alneberg et al., 2020). Like biomarker prediction, ML models were used to predict the critical bacterial sub-OTUs (s-

OTUs) associated with copepods genera. RF and GB predicted the important bacteriome associated with five different copepod genera viz., *Acartia* spp., *Calanus* spp., *Centropages* sp., *Pleuromamma* spp., and *Temora* spp... The gradient boosting classifiers predicted a total of 50 s-OTUs as important in five copepod genera. Among the predicted s-OTUs, s-OTUs representing the *Acinetobacter johnsonii*, *Phaeobacter*, *Vibrio shilonii* and Piscirickettsiaceae were reported as important s-OTUs in *Calanus* spp., and the eight s-OTUs representing *Marinobacter*, *Alteromonas*, *Desulfovibrio*, *Limnobacter*, *Sphingomonas*, *Methyloversatilis*, *Enhydrobacter* and Coriobacteriaceae were predicted as important s-OTUs in *Pleuromamma* spp., for the first time (Sadaiappan et al., 2021).

Identification of individual microbes requires sophisticated instruments, specific media composition and time. Also, it is a high risk to culture and identify pathogens related to a biological risk-related emergency. The recent development of Single-cell Raman spectroscopy (scRS) contains a 1000 Raman band, a single-cell fingerprint that represents the cells' inherent phenotype, genotype and physiological information. However, analysing scRS is challenging because it requires a sequential process that consumes time. An advanced one-dimensional CNN classification algorithm (1DCNN) proved to be an effective way to analyse scRS data to identify microbes automatically.

Along with other ML algorithms like KNN, SVM, PCA-LDA, 1DCNN accurately classified the microbes from ten actinomycetes, one non-marine actinomycete and *E.coli* (reference species) scRS dataset. 1DCNN had similar accuracy to other models (~95%), but the recall rate was higher than other models (Liu et al., 2020). Later in the classification of deep-sea microbes using Raman spectra, the addition of Progressive Growing of Generative Adversarial Nets (PGGAN) enhanced the classification accuracy. PGGAN created a spectral dataset similar to actual spectra data acquired from single-cell Raman spectra from the five deep-sea bacteria. The residual network (ResNet) accurately classified bacteria (accuracy of $99.8\pm0.2\%$) using the PGGAN dataset. The use of PGGAN proved to be an efficient data augmentation method to handle low amounts of data and categorise the spectrum with a low signal-to-noise ratio. Moreover, the model reduced the requirement of a large dataset for training data (Liu et al., 2022).

Glossary

Machine learning (ML)

Artificial intelligence (AI)

Random forest (RF)

Convolutional Neural Networks (CNN)

Reinforcement learning (RL)

Gaussian Mixture Model (GMM)

Dissolved Oxygen (DO)

Southern Ocean (SO)

Southern Ocean State Estimate (SOSE)

World Ocean Atlas (WOA13)

Marine-deep jointly informed neural network (M-DJINN)

Deep jointly informed neural network (DJINN)

Empirical wavelet transformation (EWT)

Random forest regression (RFR)

Random regression forests (RRF)

Support vector regression (SVR)

Oxygen minimum zones (OMZs)

National Ocean and Atmospheric Administration Earth System Research Laboratories
(NOAA/ESRL)

Unicellular cyanobacteria group A (UCYN-A)

Artificial neural networks (ANN)

MLP (Multilayer Perceptron)

SVM (Support Vector Machine)

Global Predictive Seabed Model (GPSM)

Random forest-based regression ensemble (RFRE)

K Nearest neighbours (KNN)

Total organic carbon (TOC)

Long Short-Term Memory neural network (LSTM)

Global Predictive Seabed Model (GPSM)

Shadow Image Particle Profiling Evaluation Recorder (SIPPER)

Greedy Feature Flip Algorithm (G-flip)

Deep convolutional neural network (DCNN)

FORaminifera roBOT (FORABOT)

MVCO IFCB

Deep convolutional network (DNN)

Multiple kernel learning (MKL)

NLMKL

Northern Adriatic Sea (NA)

Weighted average prediction error -WA-PE-

Boosted Regression Tree (BRT)

Southern Ocean (SO)

Pairwise permutational multivariate analysis of variance (PERMANOVA)

Net primary productivity (NPP)

Bermuda Atlantic Time-series Study (BATS)

Genetic programming (GP)

Phytoplankton microscopic image dataset (PMID)

Chlorophyll-a (Chl-a)

Suspended particulate matter (SPM)

Geostationary Ocean Colour Imager (GOCI)

Ocean colour net (OCN)

Gaussian process Regression (GPR),

Ocean Colour (OC3) algorithm,

Case-2 regional/coast colour (C2RCC)

Harmful algal bloom (HAB)

Linear discriminant analysis (LDA)

Neural Networks (NN)

intelligent Screening of underwater Image Sequences (iSIS)

Eastern Tropical Pacific (ETP)

Automated underwater vehicle (AUV)

Deep learning algorithms (DLA)

Remote operated vehicle (ROV)

Marine Object-Based Image Analysis (MOBIA)

Frames per second (FPS)

Multilayer Graph Regularized Extreme Learning Machine Autoencoder (MIGRATE_ELM)

Voting ensemble (VE)

In situ Ichthyoplankton Imaging System (ISIIS)

single cell Raman spectroscopy (scRS)

Linear discriminant analysis (LDA) effect size (LEfSe)

Metagenome-assembled genomes (MAG)

Broyden–Fletcher–Goldfarb–Shanno (BFGS), Extended Nearest Neighbor (ENN), General Regression Neural Network -(GRNN), Outlier Robust Extreme Learning Machine -(ORELM), and Extreme Learning Machine -(ELM) are combined to obtain the BEGOE model.

References

1. Adam O., Lopatka M., Laplanche C., Motsch J.-F., 2005. Sperm whale signal analysis: comparison using the autoregressive model and the wavelet transform. *World Academy of Science, Engineering and Technology*, 4, pp. 188-195.
2. Ahmad, H. (2019). Machine Learning Applications in Oceanography. *Aquatic Research*, 161–169. <https://doi.org/10.3153/ar19014>.
3. Allken, V., Handegard, N. O., Rosen, S., Schreyeck, T., Mahiout, T., & Malde, K. (2019). Fish species identification using a convolutional neural network trained on synthetic data. *ICES Journal of Marine Science*, 76(1), 342–349. <https://doi.org/10.1093/icesjms/fsy147>.
4. Alneberg, J., Bennke, C., Beier, S., Bunse, C., Quince, C., Ininbergs, K., Riemann, L., Ekman, M., Jürgens, K., Labrenz, M., Pinhassi, J., & Andersson, A. F. (2020). Ecosystem-wide metagenomic binning enables prediction of ecological niches from genomes. *Communications Biology*, 3(1), 1–10. <https://doi.org/10.1038/s42003-020-0856-x>.
5. Álvarez, E., López-Urrutia, Á., & Nogueira, E. (2012). Improvement of plankton biovolume estimates derived from image-based automatic sampling devices: application to FlowCAM. *Journal of Plankton Research*, 34(6), 454–469. <https://doi.org/10.1093/plankt/fbs017>.
6. Álvarez, E., López-Urrutia, Á., Nogueira, E., 2012. Improvement of plankton biovolume estimates derived from image-based automatic sampling devices: Application to Flowcam. *Journal of Plankton Research* 34, 454–469. doi:10.1093/plankt/fbs017
7. Álvarez, E., Moyano, M., López-Urrutia, Á., Nogueira, E., & Scharek, R. (2014). Routine determination of plankton community composition and size structure: A comparison

- between FlowCAM and light microscopy. *Journal of Plankton Research*, 36(1), 170–184. <https://doi.org/10.1093/plankt/fbt069>.
8. Álvarez, E., Moyano, M., López-Urrutia, Á., Nogueira, E., Scharek, R., 2013. Routine determination of plankton community composition and size structure: A comparison between Flowcam and light microscopy. *Journal of Plankton Research* 36, 170–184. doi:10.1093/plankt/fbt069.
 9. Anderson, D. M., Cembella, A. D., & Hallegraeff, G. M. (2012). Progress in understanding harmful algal blooms: Paradigm shifts and new technologies for research, monitoring, and Management. *Annual Review of Marine Science*, 4(1), 143–176. <https://doi.org/10.1146/annurev-marine-120308-081121>.
 10. Asim, M., Brekke, C., Mahmood, A., Eltoft, T., & Reigstad, M. (2021). Improving Chlorophyll-A Estimation From Sentinel-2 (MSI) in the Barents Sea Using Machine Learning. *IEEE Journal of Selected Topics in Applied Earth Observations and Remote Sensing*, 14, 5529–5549. <https://doi.org/10.1109/jstars.2021.3074975>.
 11. Aya Saad, A. S., Andreas Våge, Emlyn Davies, Tor Nordam, N. A., Martin Ludvigsen, Geir Johnsen, João Sousa, and K. R. (2020). Advancing Ocean Observation with an AI-Driven Mobile Robotic Explorer. *Oceanography*, 33(3), 50-59.
 12. Bell, J.L., Hopcroft, R.R., 2008. Assessment of zoimage as a tool for the classification of Zooplankton. *Journal of Plankton Research* 30, 1351–1367. doi:10.1093/plankt/fbn092
 13. Benfield, M., Grosjean, P., Culverhouse, P., Irigolen, X., Sieracki, M., Lopez-Urrutia, A., Dam, H., Hu, Q., Davis, C., Hanson, A., Pilskaln, C., Riseman, E., Schulz, H., Utgoff, P., Gorsky, G., 2007. Rapid: Research on automated plankton identification. *Oceanography* 20, 172–187. doi:10.5670/oceanog.2007.63
 14. Bermant, P. C., Bronstein, M. M., Wood, R. J., Gero, S., & Gruber, D. F. (2019). Deep Machine Learning Techniques for the Detection and Classification of Sperm Whale Bioacoustics. *Scientific Reports*, 9(1), 1–10. <https://doi.org/10.1038/s41598-019-48909-4>.
 15. Bombar, D., Paerl, R. W., & Riemann, L. (2016). Marine Non-Cyanobacterial Diazotrophs: Moving beyond Molecular Detection. In *Trends in Microbiology* (Vol. 24, Issue 11, pp. 916–927). Elsevier BV. <https://doi.org/10.1016/j.tim.2016.07.002>
 16. Bors, E. K., Baker, C. S., Wade, P. R., O'Neill, K. B., Sheldon, K. E. W., Thompson, M. J., Fei, Z., Jarman, S., & Horvath, S. (2021). An epigenetic clock to estimate the age of living beluga whales. *Evolutionary Applications*, 14(5), 1263–1273. <https://doi.org/10.1111/eva.13195>.

17. Bourel, M., Crisci, C., & Martínez, A. (2017). Consensus methods based on machine learning techniques for marine phytoplankton presence–absence prediction. *Ecological Informatics*, 42, 46–54. <https://doi.org/10.1016/j.ecoinf.2017.09.004>.
18. Bradbury, H. J., & Turchyn, A. V. (2019). Reevaluating the carbon sink due to sedimentary carbonate formation in modern marine sediments. *Earth and Planetary Science Letters*, 519, 40–49. <https://doi.org/10.1016/j.epsl.2019.04.044>.
19. Breitburg, D., Levin, L. A., Oschlies, A., Grégoire, M., Chavez, F. P., Conley, D. J., Garçon, V., Gilbert, D., Gutiérrez, D., Isensee, K., Jacinto, G. S., Limburg, K. E., Montes, I., Naqvi, S. W., Pitcher, G. C., Rabalais, N. N., Roman, M. R., Rose, K. A., Seibel, B. A., ... Zhang, J. (2018). Declining oxygen in the global ocean and Coastal Waters. *Science*, 359(6371). <https://doi.org/10.1126/science.aam7240>.
20. Brewster, L. R., Dale, J. J., Guttridge, T. L., Gruber, S. H., Hansell, A. C., Elliott, M., Cowx, I. G., Whitney, N. M., & Gleiss, A. C. (2018). Development and application of a machine learning algorithm for classification of elasmobranch behaviour from accelerometry data. *Marine Biology*, 165(4), 1–19. <https://doi.org/10.1007/s00227-018-3318-y>.
21. Briseño-Avena, C., Schmid, M.S., Swieca, K., Sponaugle, S., Brodeur, R.D., Cowen, R.K., 2020. Three-dimensional cross-shelf zooplankton distributions off the central Oregon coast during anomalous oceanographic conditions. *Progress in Oceanography* 188, 102436. doi:10.1016/j.pocean.2020.102436.
22. Buongiorno Nardelli, B. (2020). A Deep Learning Network to Retrieve Ocean Hydrographic Profiles from Combined Satellite and *In situ* Measurements. In *Remote Sensing* (Vol. 12, Issue 19, p. 3151). MDPI AG. <https://doi.org/10.3390/rs12193151>.
23. Cai, R., Han, T., Liao, W., Huang, J., Li, D., Kumar, A., & Ma, H. (2020). Prediction of surface chloride concentration of marine concrete using ensemble machine learning. *Cement and Concrete Research*, 136 (July 2019), 106164. <https://doi.org/10.1016/j.cemconres.2020.106164>.
24. Chen, L., Xu, S., Gao, Z., Chen, H., Zhang, Y., Zhan, J., Li, W., 2011. Estimation of monthly air-Sea CO₂ flux in the Southern Atlantic and Indian Ocean using in-situ and remotely sensed data. *Remote Sensing of Environment* 115, 1935–1941. doi:10.1016/j.rse.2011.03.016
25. Chen, S., Hu, C., Barnes, B.B., Wanninkhof, R., Cai, W.-J., Barbero, L., Pierrot, D., 2019. A machine learning approach to estimate surface ocean PCO₂ from satellite measurements. *Remote Sensing of Environment* 228, 203–226. doi:10.1016/j.rse.2019.04.019

26. Cheng, K., Cheng, X., Wang, Y., Bi, H., & Benfield, M. C. (2019). Enhanced convolutional neural network for plankton identification and enumeration. *PLoS ONE*, 14(7), 1–17. <https://doi.org/10.1371/journal.pone.0219570>.
27. Cheng, X., Ren, Y., Cheng, K., Cao, J., Hao, Q., 2020. Method for training convolutional neural networks for *in situ* plankton image recognition and classification based on the mechanisms of the human eye. *Sensors* 20, 2592. doi:10.3390/s20092592.
28. Conti, L. A., Lim, A., & Wheeler, A. J. (2019). High resolution mapping of a cold water coral mound. *Scientific Reports*, 9(1), 1–15. <https://doi.org/10.1038/s41598-018-37725-x>.
29. Cooper, K. M., & Barry, J. (2020). A new machine learning approach to seabed biotope classification. *Ocean & Coastal Management*, 198, 105361. <https://doi.org/10.1016/j.ocecoaman.2020.105361>.
30. Costello, M. J., & Chaudhary, C. (2017). Marine Biodiversity, biogeography, deep-sea gradients, and conservation. *Current Biology*, 27(11). <https://doi.org/10.1016/j.cub.2017.04.060>
31. Cui, S., Zhou, Y., Wang, Y. and Zhai, L., (2020). Fish detection using deep learning. *Applied Computational Intelligence and Soft Computing*, 2020. DOI: 10.1155/2020/3738108.
32. Culverhouse PF, Ellis RE, Simpson R, Williams R, Pierce RW, Turner JT (1994) Categorisation of five species of Cymato-cylis (Tintinidae) by artificial neural network. *Mar Ecol Prog Ser* 107:273–280.
33. D'Alelio, D., Rampone, S., Cusano, L. M., Morfino, V., Russo, L., Sanseverino, N., Cloern, J. E., & Lomas, M. W. (2020). Machine learning identifies a strong association between warming and reduced primary productivity in an oligotrophic ocean gyre. *Scientific Reports*, 10(1), 1–12. <https://doi.org/10.1038/s41598-020-59989-y>.
34. Dai, J., Wang, R., Zheng, H., Ji, G., & Qiao, X. (2016). ZooplanktoNet: Deep Convolutional Network for Zooplankton classification. *OCEANS 2016 - Shanghai*. <https://doi.org/10.1109/oceansap.2016.7485680>.
35. Davis CS, Hu Q, Gallager SM, Tang X, Ashjian CJ (2004) Real-time observation of taxa-specific plankton distributions: an optical sampling method. *Mar Ecol Prog Ser* 284:77–96.
36. Delmont, T. O., Quince, C., Shaiber, A., Esen, Ö. C., Lee, S. T. M., Rappé, M. S., McLellan, S. L., Lückner, S., & Eren, A. M. (2018). Nitrogen-fixing populations of Planctomycetes and proteobacteria are abundant in surface ocean metagenomes. *Nature Microbiology*, 3(7), 804–813. <https://doi.org/10.1038/s41564-018-0176-9>.

37. Demertzis, K., Iliadis, L. S., & Anezakis, V. D. (2018). Extreme deep learning in biosecurity: The case of machine hearing for marine species identification. *Journal of Information and Telecommunication*, 2(4), 492–510. <https://doi.org/10.1080/24751839.2018.1501542>.
38. Demertzis, K., Iliadis, L., Anezakis, V.-D., 2017. A deep spiking machine-hearing system for the case of invasive fish species. 2017 IEEE International Conference on INnovations in Intelligent SysTems and Applications (INISTA). doi:10.1109/inista.2017.8001126
39. Denvil-Sommer, A., Gehlen, M., Vrac, M., Mejia, C., 2019. LSCE-FFNN-V1: A two-step neural network model for the reconstruction of Surface Ocean <I>pCO₂ over the Global Ocean. *Geoscientific Model Development* 12, 2091–2105. doi:10.5194/gmd-12-2091-2019 .
40. Deutsch, C., Sarmiento, J.L., Sigman, D.M., Gruber, N., Dunne, J.P., 2007. Spatial coupling of nitrogen inputs and losses in the Ocean. *Nature* 445, 163–167. doi:10.1038/nature05392
41. Diao, Y., Yan, L., & Gao, K. (2021). Improvement of the machine learning-based corrosion rate prediction model through the optimization of input features. *Materials and Design*, 198, 109326. <https://doi.org/10.1016/j.matdes.2020.109326>.
42. Diaz, R. J., & Rosenberg, R. (2008). Spreading Dead Zones and Consequences for Marine Ecosystems. In *Science* (Vol. 321, Issue 5891, pp. 926–929). American Association for the Advancement of Science (AAAS). <https://doi.org/10.1126/science.1156401>.
43. Diouf, D., & Seck, D. (2019). Modeling the Chlorophyll-a from Sea Surface Reflectance in West Africa by Deep Learning Methods: A Comparison of Multiple Algorithms. *International Journal of Artificial Intelligence & Applications*, 10(6), 33–40. <https://doi.org/10.5121/ijaia.2019.10603>.
44. Ellen, J., Li, H., & Ohman, M. D. (2016). Quantifying California current plankton samples with efficient machine learning techniques. *OCEANS 2015 - MTS/IEEE Washington*. <https://doi.org/10.23919/oceans.2015.7404607>.
45. Ellen, J., Hongyu Li, Ohman, M.D., 2015. Quantifying California current plankton samples with Efficient Machine Learning Techniques. *OCEANS 2015 - MTS/IEEE Washington*. doi:10.23919/oceans.2015.7404607.
46. Eymold, W. K., Frederick, J. M., Nole, M., Phrampus, B. J., & Wood, W. T. (2021). Prediction of Gas Hydrate Formation at Blake Ridge Using Machine Learning and Probabilistic Reservoir Simulation. In *Geochemistry, Geophysics, Geosystems* (Vol. 22, Issue 4). American Geophysical Union (AGU). <https://doi.org/10.1029/2020gc009574>.

47. Faillettaz, R., Picheral, M., Luo, J., Guigand, C., Cowen, R., Irisson, J.-O., 2016. Imperfect automatic image classification successfully describes plankton distribution patterns. *Methods in Oceanography* 15-16, 60–77. doi:10.1016/j.mio.2016.04.003.
48. Falkowski, P., 2012. Ocean science: The power of plankton. *Nature* 483. doi:10.1038/483s17a.
49. Feuilloley, G., Fromentin, J.-M., Saraux, C., Irisson, J.-O., Jalabert, L., Stemmann, L., 2021. Temporal fluctuations in zooplankton size, abundance, and taxonomic composition since 1995 in the North Western Mediterranean Sea. *ICES Journal of Marine Science* 79, 882–900. doi:10.1093/icesjms/fsab190.
50. Flombaum, P., Wang, W. L., Primeau, F. W., & Martiny, A. C. (2020). Global picophytoplankton niche partitioning predicts overall positive response to ocean warming. *Nature Geoscience*, 13(2), 116–120. <https://doi.org/10.1038/s41561-019-0524-2>.
51. Francisco Caio Maia Rodrigues¹, Nina S. T. Hirata¹, Antonio A. Abello¹, Leandro T. De La Cruz¹, R. M. L. and R. H. J., & Hirata, R. (2018). Evaluation of transfer learning scenarios in plankton image classification. *VISIGRAPP 2018 - Proceedings of the 13th International Joint Conference on Computer Vision, Imaging and Computer Graphics Theory and Applications*, 5 (Visigrapp), 359–366. <https://doi.org/10.5220/0006626703590366>.
52. Friedrich, T., Oeschies, A., 2009. Basin-scale PCO₂ maps estimated from Argo Float Data: A model study. *Journal of Geophysical Research* 114. doi:10.1029/2009jc005322.
53. Friedrich, T., Oeschies, A., 2009. Neural network-based estimates of North Atlantic surface PCO₂ from satellite data: A methodological study. *Journal of Geophysical Research* 114. doi:10.1029/2007jc004646.
54. Fullgrabe, L., Grosjean, P., Gobert, S., Lejeune, P., Leduc, M., Engels, G., Dauby, P., Boissery, P., Richir, J., 2020. Zooplankton dynamics in a changing environment: A 13-year survey in the northwestern Mediterranean Sea. *Marine Environmental Research* 159, 104962. doi:10.1016/j.marenvres.2020.104962.
55. Gaetz, W., Jantzen, K., Weinberg, H., Spong, P., & Symonds, H. (n.d.). A neural network method for recognition of individual *Orcinus orca* based on their acoustic behaviour: phase 1. In *Proceedings of OCEANS '93. OCEANS '93. IEEE*. <https://doi.org/10.1109/oceans.1993.325960>.

56. Gerhard, W. A., & Gunsch, C. K. (2019). Metabarcoding and machine learning analysis of environmental DNA in ballast water arriving at hub ports. *Environment International*, 124(December 2018), 312–319. <https://doi.org/10.1016/j.envint.2018.12.038>.
57. Giglio, D., Lyubchich, V., & Mazloff, M. R. (2018). Estimating Oxygen in the Southern Ocean Using Argo Temperature and Salinity. *Journal of Geophysical Research: Oceans*, 123(6), 4280–4297. <https://doi.org/10.1029/2017jc013404>.
58. González, P., Castaño, A., Peacock, E. E., Díez, J., Del Coz, J. J., & Sosik, H. M. (2019). Automatic plankton quantification using deep features. *Journal of Plankton Research*, 41(4), 449–463. <https://doi.org/10.1093/plankt/fbz023>.
59. Gorocs, Z., Tamamitsu, M., Bianco, V., Wolf, P., Roy, S., Shindo, K., Yanny, K., Wu, Y., Koydemir, H. C., Rivenson, Y., & Ozcan, A. (2018). A deep learning-enabled portable imaging flow cytometer for cost-effective, high-throughput, and label-free analysis of natural water samples. *Light: Science and Applications*, 7(1), 1–12. <https://doi.org/10.1038/s41377-018-0067-0>.
60. Gorsky, G., Ohman, M. D., Picheral, M., Gasparini, S., Stemmann, L., Romagnan, J. B., Cawood, A., Pesant, S., García-Comas, C., & Prejger, F. (2010). Digital zooplankton image analysis using the ZooScan integrated system. *Journal of Plankton Research*, 32(3), 285–303. <https://doi.org/10.1093/plankt/fbp124>.
61. Grosjean, P. and Denis, K. (2007) ZooImage Users Manual
62. Guirado, E., Tabik, S., Rivas, M. L., Alcaraz-Segura, D., & Herrera, F. (2019). Whale counting in satellite and aerial images with deep learning. *Scientific Reports*, 9(1), 1–12. <https://doi.org/10.1038/s41598-019-50795-9>.
63. gwon, S., & Bushinsky, S. (2014). Oxygen concentrations and biological fluxes in the Open Ocean. *Oceanography*, 27(1), 168–171. <https://doi.org/10.5670/oceanog.2014.20>
64. Hafeez, S., Wong, M., Ho, H., Nazeer, M., Nichol, J., Abbas, S., Tang, D., Lee, K., Pun, L., 2019. Comparison of machine learning algorithms for retrieval of water quality indicators in case-II waters: A case study of hong kong. *Remote Sensing* 11, 617. doi:10.3390/rs11060617
65. Hales, B., Strutton, P.G., Saraceno, M., Letelier, R., Takahashi, T., Feely, R., Sabine, C., Chavez, F., 2012. Satellite-based prediction of PCO₂ in coastal waters of the eastern North Pacific. *Progress in Oceanography* 103, 1–15. doi:10.1016/j.pocean.2012.03.001.

66. Han, F., Yao, J., Zhu, H., & Wang, C. (2020). Marine Organism Detection and Classification from Underwater Vision Based on the Deep CNN Method. *Mathematical Problems in Engineering*, 1-11. <https://doi.org/10.1155/2020/3937580>.
67. Han, F., Yao, J., Zhu, H., & Wang, C. (2020). Underwater Image Processing and Object Detection Based on Deep CNN Method. *Journal of Sensors*, 2020, 1–20. <https://doi.org/10.1155/2020/6707328>.
68. He, J., Chen, Y., Wu, J., Stow, D.A., Christakos, G., 2020. Space-time chlorophyll-a retrieval in optically complex waters that accounts for remote sensing and modeling uncertainties and improves remote estimation accuracy. *Water Research* 171, 115403. doi:10.1016/j.watres.2019.115403.
69. Henley, S. F., Cavan, E. L., Fawcett, S. E., Kerr, R., Monteiro, T., Sherrell, R. M., Bowie, A. R., Boyd, P. W., Barnes, D. K., Schloss, I. R., Marshall, T., Flynn, R., & Smith, S. (2020). Changing biogeochemistry of the Southern Ocean and its ecosystem implications. *Frontiers in Marine Science*, 7. <https://doi.org/10.3389/fmars.2020.00581>.
70. Hsiao, Y.-H., Chen, C.-C., Lin, S.-I., Lin, F.-P., 2014. Real-world underwater fish recognition and identification, using sparse representation. *Ecological Informatics* 23, 13–21. doi:10.1016/j.ecoinf.2013.10.002.
71. Hski, M., Chazottes, A., Schuster, U., Watson, A.J., Moulin, C., Bakker, D.C., González-Dávila, M., Johannessen, T., Körtzinger, A., Lüger, H., Olsen, A., Omar, A., Padin, X.A., Ríos, A.F., Steinhoff, T., Santana-Casiano, M., Wallace, D.W., Wanninkhof, R., 2009. Estimating the monthly *pco2* distribution in the North Atlantic using a self-organizing neural network. *Biogeosciences* 6, 1405–1421. doi:10.5194/bg-6-1405-2009.
72. Hu, C., Feng, L., & Guan, Q. (2021). A machine learning approach to estimate surface chlorophyll a concentration in global oceans from satellite measurements. *IEEE Transactions on Geoscience and Remote Sensing*, 59(6), 4590–4607. <https://doi.org/10.1109/tgrs.2020.3016473>.
73. Hu, C., Lee, Z., & Franz, B. (2012). Chlorophyll algorithms for oligotrophic oceans: A novel approach based on three-band Reflectance Difference. *Journal of Geophysical Research: Oceans*, 117(C1). <https://doi.org/10.1029/2011jc007395>.
74. Hu, Q., Davis, C., 2005. Automatic plankton image recognition with co-occurrence matrices and support vector machine. *Marine Ecology Progress Series* 295, 21–31. doi:10.3354/meps295021.

75. Huynh, Q.Q., Cooper, L.N., Intrator, N., Shouval, H., 1998. Classification of underwater mammals using feature extraction based on time-frequency analysis and BCM theory. *IEEE Transactions on Signal Processing* 46, 1202–1207. doi:10.1109/78.668783
76. Jamet, C., Moulin, C., Lefèvre, N., 2007. Estimation of the oceanic pco₂ in the North Atlantic from VOS lines in-situ measurements: Parameters needed to generate seasonally mean maps. *Annales Geophysicae* 25, 2247–2257. doi:10.5194/angeo-25-2247-2007
77. Jeffries, H. P., Sherman , K., Maurer , R., et al., & Kennedy , V. (1980). Computer processing of zooplankton samples. In *Estuarine Perspectives* (pp. 303–316). essay, New York Academic Press.
78. Jeffries, H.P., Berman, M.S., Poularikas, A.D., Katsinis, C., Melas, I., Sherman, K., Bivins, L., 1984. Automated sizing, counting and identification of zooplankton by pattern recognition. *Marine Biology* 78, 329–334. doi:10.1007/bf00393019.
79. Jin, D., Lee, E., Kwon, K., & Kim, T. (2021). A Deep Learning Model Using Satellite Ocean Color and Hydrodynamic Model to Estimate Chlorophyll-a Concentration. *Remote Sensing*, 13(10), 2003. <https://doi.org/10.3390/rs13102003>.
80. Jo, Y.-H., Dai, M., Zhai, W., Yan, X.-H., Shang, S., 2012. On the variations of sea surface pco₂ in the northern South China Sea: A Remote Sensing based neural network approach. *Journal of Geophysical Research: Oceans* 117. doi:10.1029/2011jc007745.
81. Johnson, K.S., Coale, K.H., Jannasch, H.W., 1992. Analytical Chemistry in Oceanography. *Analytical Chemistry* 64. doi:10.1021/ac00046a715.
82. Kerr, T., Clark, J. R., Fileman, E. S., Widdicombe, C. E., & Pugeault, N. (2020). Collaborative Deep Learning Models to Handle Class Imbalance in FlowCam Plankton Imagery. In *IEEE Access* (Vol. 8, pp. 170013–170032). Institute of Electrical and Electronics Engineers (IEEE). <https://doi.org/10.1109/access.2020.3022242>.
83. Kim, Y. H., Im, J., Ha, H. K., Choi, J. K., & Ha, S. (2014). Machine learning approaches to coastal water quality monitoring using GOCI satellite data. *GIScience and Remote Sensing*, 51(2), 158–174. <https://doi.org/10.1080/15481603.2014.900983>.
84. Kim, D. K., Jeong, K. S., McKay, R. I. B., Chon, T. S., & Joo, G. J. (2012). Machine learning for predictive management: Short and long term prediction of phytoplankton

- biomass using genetic algorithm based recurrent neural networks. *International Journal of Environmental Research*, 6 (1), 95–108.
85. Kleppel, G., Burkart C. 1995. Egg production and the nutritional environment of *Acartia tonsa*: The role of food quality in copepod nutrition. *ICES Journal of Marine Science* 52, 297–304. doi:10.1016/1054-3139(95)80045-x.
 86. Kloster, M., Langenkämper, D., Zurowietz, M., Beszteri, B., & Nattkemper, T. W. (2020). Deep learning-based diatom taxonomy on virtual slides. *Scientific Reports*, 10 (1), 1–13. <https://doi.org/10.1038/s41598-020-71165-w>.
 87. Lalli, C.M., Parsons, T.R., 1999. Biological oceanography: An introduction. Butterworth-Heinemann.
 88. Langenkämper, D., Simon-Lledó, E., Hosking, B., Jones, D. O. B., & Nattkemper, T. W. (2019). On the impact of Citizen Science-derived data quality on deep learning based classification in marine images. *PLoS ONE*, 14(6), 1–16. <https://doi.org/10.1371/journal.pone.0218086>.
 89. Lee, H., Park, M., & Kim, J. (2016). Plankton classification on an imbalanced large scale database via convolutional neural networks with transfer learning. *Proceedings - International Conference on Image Processing, ICIP, 2016*, 3713–3717. <https://doi.org/10.1109/ICIP.2016.7533053>.
 90. Lee, T. R., Wood, W. T., & Phrampus, B. J. (2019). A Machine Learning (kNN) Approach to Predicting Global Seafloor Total Organic Carbon. *Global Biogeochemical Cycles*, 33(1), 37–46. <https://doi.org/10.1029/2018GB005992>.
 91. Lefèvre, N., Watson, A.J., Watson, A.R., 2005. A comparison of multiple regression and neural network techniques for mapping *in situ* PCO₂ data. *Tellus B: Chemical and Physical Meteorology* 57, 375–384. doi:10.3402/tellusb.v57i5.16565.
 92. Li, Q., Sun, X., Dong, J., Song, S., Zhang, T., Liu, D., Zhang, H., & Han, S. (2020). Developing a microscopic image dataset in support of intelligent phytoplankton detection using deep learning. *ICES Journal of Marine Science*, 77(4), 1427–1439. <https://doi.org/10.1093/icesjms/fsz171>.
 93. Li, Y., Guo, J., Guo, X., Hu, Z., & Tian, Y. (2021). Plankton Detection with Adversarial Learning and a Densely Connected Deep Learning Model for Class Imbalanced Distribution. In *Journal of Marine Science and Engineering* (Vol. 9, Issue 6, p. 636). MDPI AG. <https://doi.org/10.3390/jmse9060636>.

94. Liu, B., Liu, K., Wang, N., Ta, K., Liang, P., Yin, H., Li, B., 2022. Laser tweezers Raman spectroscopy combined with deep learning to classify marine bacteria. *Talanta* 244, 123383. doi:10.1016/j.talanta.2022.123383.
95. Liu, H., Yang, R., Duan, Z., & Wu, H. (2021). A hybrid neural network model for marine dissolved oxygen concentrations time-series forecasting based on multi-factor analysis and a multi-model ensemble. *Engineering*. <https://doi.org/10.1016/j.eng.2020.10.023>.
96. Liu, L., Yang, H., Cai, Y., Cao, Q., Sun, L., Wang, Z., Li, W., Liu, G., Lee, P. W., & Tang, Y. (2019). In silico prediction of chemical aquatic toxicity for marine crustaceans via machine learning. *Toxicology Research*, 8(3), 341–352. <https://doi.org/10.1039/c8tx00331a>.
97. Liu, P., Li, Y., Liu, B., Chen, P., & Xu, J. (2019). Semi-automatic oil spill detection on X-band marine radar images using texture analysis, machine learning, and adaptive thresholding. *Remote Sensing*, 11(7). <https://doi.org/10.3390/rs11070756>.
98. Liu, X., Jia, Z., Hou, X., Fu, M., Ma, L., & Sun, Q. (2019). Real-time marine animal images classification by embedded system based on Mobilenet and Transfer Learning. *OCEANS 2019 - Marseille*. <https://doi.org/10.1109/oceanse.2019.8867190>.
99. Liu, Y., Xu, J., Tao, Y., Fang, T., Du, W., & Ye, A. (2020). Rapid and accurate identification of marine microbes with single-cell Raman spectroscopy. *Analyst*, 145(9), 3297–3305. <https://doi.org/10.1039/c9an02069a>.
100. Lohrenz, S.E., Cai, W.-J., Chakraborty, S., Huang, W.-J., Guo, X., He, R., Xue, Z., Fennel, K., Howden, S., Tian, H., 2018. Satellite estimation of coastal PCO₂ and air-sea flux of carbon dioxide in the northern Gulf of Mexico. *Remote Sensing of Environment* 207, 71–83. doi:10.1016/j.rse.2017.12.039.
101. Lopatka, M., Adam, O., Laplanche, C., Zarzycki, J., Motsch, J.-F., 2005. An attractive alternative for sperm whale click detection using the wavelet transform in comparison to the Fourier spectrogram. *Aquatic Mammals* 31, 463–467. doi:10.1578/am.31.4.2005.463
102. Lumini, A., Nanni, L., & Maguolo, G. (2020). Deep learning for plankton and coral classification. *Applied Computing and Informatics*, xxxx. <https://doi.org/10.1016/j.aci.2019.11.004>.
103. Luo, J. Y., Irisson, J. O., Graham, B., Guigand, C., Sarafranz, A., Mader, C., & Cowen, R. K. (2018). Automated plankton image analysis using convolutional neural networks. *Limnology and Oceanography: Methods*, 16(12), 814–827. <https://doi.org/10.1002/lom3.10285>.
104. Luo, T., Kramer, K., Goldgof, D. B., Hall, L. O., Samson, S., Remsen, A., & Hopkins, T. (2004). Recognizing plankton images from tD shadow image particle profiling

- evaluation recorder. *IEEE Transactions on Systems, Man, and Cybernetics, Part B: Cybernetics*, 34(4), 1753–1762. <https://doi.org/10.1109/TSMCB.2004.830340>.
105. Luo, Y.-W., Doney, S. C., Anderson, L. A., Benavides, M., Berman-Frank, I., Bode, A., Bonnet, S., Boström, K. H., Böttjer, D., Capone, D. G., Carpenter, E. J., Chen, Y. L., Church, M. J., Dore, J. E., Falcón, L. I., Fernández, A., Foster, R. A., Furuya, K., Gómez, F., ... Zehr, J. P. (2012). Database of diazotrophs in global ocean: abundance, biomass and nitrogen fixation rates. In *Earth System Science Data* (Vol. 4, Issue 1, pp. 47–73). Copernicus GmbH. <https://doi.org/10.5194/essd-4-47-2012>.
 106. Luo, Y.-W., Doney, S. C., Anderson, L. A., Benavides, M., Berman-Frank, I., Bode, A., Bonnet, S., Boström, K. H., Böttjer, D., Capone, D.G., Carpenter, E. J., Chen, Y. L., Church, M. J., Dore, J. E., Falcón, L. I., Fernández, A., Foster, R. A., Furuya, K., Gómez, F., ... Zehr, J. P. (2012). Database of diazotrophs in global ocean: abundance, biomass and nitrogen fixation rates. In *Earth System Science Data* (Vol. 4, Issue 1, pp. 47–73). Copernicus GmbH. <https://doi.org/10.5194/essd-4-47-2012>.
 107. Luo, Y.-W., Lima, I. D., Karl, D. M., Deutsch, C. A., & Doney, S. C. (2014). Data-based assessment of environmental controls on global marine nitrogen fixation. *Biogeosciences*, 11(3), 691–708. <https://doi.org/10.5194/bg-11-691-2014>.
 108. Marrec, P., Cariou, T., Macé, E., Morin, P., Salt, L.A., Vernet, M., Taylor, B., Paxman, K., Bozec, Y., 2015. Dynamics of air–sea co2 Fluxes in the northwestern European shelf based on voluntary observing ship and satellite observations. *Biogeosciences* 12, 5371–5391. doi:10.5194/bg-12-5371-2015
 109. Martinez, E., Brini, A., Gorgues, T., Drumetz, L., Roussillon, J., Tandeo, P., Maze, G., & Fablet, R. (2020b). Neural network approaches to reconstruct phytoplankton time-series in the global ocean. *Remote Sensing*, 12(24), 1–13. <https://doi.org/10.3390/rs12244156>.
 110. Martinez, E., Gorgues, T., Lengaigne, M., Fontana, C., Sauzède, R., Menkes, C., Uitz, J., Di Lorenzo, E., & Fablet, R. (2020a). Reconstructing Global Chlorophyll-a Variations Using a Non-linear Statistical Approach. *Frontiers in Marine Science*, 7. <https://doi.org/10.3389/fmars.2020.00464>.
 111. Mitra, R., Marchitto, T. M., Ge, Q., Zhong, B., Kanakiya, B., Cook, M. S., Fehrenbacher, J. S., Ortiz, J. D., Tripathi, A., & Lobaton, E. (2019). Automated species-level identification of planktic foraminifera using convolutional neural networks, with comparison to human performance. *Marine Micropaleontology*, 147(January), 16–24. doi.org/10.1016/j.marmicro.2019.01.005.

112. Møhl, B., Wahlberg, M., Madsen, P.T., Heerfordt, A., Lund, A., 2003. The monopulsed nature of sperm whale clicks. *The Journal of the Acoustical Society of America* 114, 1143–1154. doi:10.1121/1.1586258
113. Moitinho-Silva, L., Steinert, G., Nielsen, S., Hardoim, C. C. P., Wu, Y. C., McCormack, G. P., López-Legentil, S., Marchant, R., Webster, N., Thomas, T., & Hentschel, U. (2017). Predicting the HMA-LMA status in marine sponges by machine learning. *Frontiers in Microbiology*, 8 (MAY), 1–14. <https://doi.org/10.3389/fmicb.2017.00752>.
114. Moussa, H., Benallal, M.A., Goyet, C., Lefèvre, N., 2016. Satellite-derived CO₂ fugacity in surface seawater of the tropical Atlantic Ocean using a Feedforward Neural Network. *International Journal of Remote Sensing* 37, 580–598. doi:10.1080/01431161.2015.1131872.
115. Muñoz, O., Rodríguez, J. G., Revilla, M., Laza-Martínez, A., Seoane, S., & Franco, J. (2020). Inhomogeneity detection in phytoplankton time series using multivariate analyses. *Oceanologia*, 62(3), 243–254. <https://doi.org/10.1016/j.oceano.2020.01.004>.
116. Murray, S. O., Mercado, E., & Roitblat, H. L. (1998). The neural network classification of false killer whale (*Pseudorca crassidens*) vocalizations. In *The Journal of the Acoustical Society of America* (Vol. 104, Issue 6, pp. 3626–3633). Acoustical Society of America (ASA). <https://doi.org/10.1121/1.423945>.
117. Naafs, B. D. A., Monteiro, F. M., Pearson, A., Higgins, M. B., Pancost, R. D., & Ridgwell, A. (2019). Fundamentally different global marine nitrogen cycling in response to severe ocean deoxygenation. In *Proceedings of the National Academy of Sciences* (Vol. 116, Issue 50, pp. 24979–24984). Proceedings of the National Academy of Sciences. <https://doi.org/10.1073/pnas.1905553116>.
118. Nakaoka, S., Telszewski, M., Nojiri, Y., Yasunaka, S., Miyazaki, C., Mukai, H., Usui, N., 2013. Estimating temporal and spatial variation of Ocean Surface pCO₂ in the North Pacific using a self-organizing map neural network technique. *Biogeosciences* 10, 6093–6106. doi:10.5194/bg-10-6093-2013.
119. Ono, T., Saino, T., Kurita, N., Sasaki, K., 2004. Basin-scale extrapolation of shipboard PCO₂ data by using satellite SST and CHL_a. *International Journal of Remote Sensing* 25, 3803–3815. doi:10.1080/01431160310001657515

120. Orenstein, E.C., Beijbom, O., 2017. Transfer learning and deep feature extraction for planktonic image data sets. 2017 IEEE Winter Conference on Applications of Computer Vision (WACV).doi:10.1109/wacv.2017.125.
121. P. Grosjean, M. Picheral, C. Warembourg and G. Gorsky, "Enumeration measurement and identification of net zooplankton samples using the zooscan digital imaging system", *ICES Journal of Marine Science*, vol. 61, no. 4, pp. 518-525, 2004.
122. Phan, T. T. H., Caillault, E. P., & Bigand, A. (2016). The identification of phytoplankton species has a high potential for monitoring environmental, climate changes. *2016 IEEE 6th International Conference on Communications and Electronics, IEEE ICCE 2016*, 283–288.<https://doi.org/10.1109/CCE.2016.7562650>.
123. Piechaud, N., Hunt, C., Culverhouse, P. F., Foster, N. L., & Howell, K. L. (2019). Automated identification of benthic epifauna with computer vision. *Marine Ecology Progress Series*, 615, 15–30. <https://doi.org/10.3354/meps12925>.
124. Pinkerton, M. H., Décima, M., Kitchener, J. A., Takahashi, K. T., Robinson, K. V., Stewart, R., & Hosie, G. W. (2020). Zooplankton in the Southern Ocean from the continuous plankton recorder: Distributions and long-term change. *Deep Sea Research Part I: Oceanographic Research Papers*, 162, 103303. <https://doi.org/10.1016/j.dsr.2020.103303>.
125. Py, O., Hong, H., & Zhongzhi, S. (2016). Plankton classification with deep convolutional neural networks. *Proceedings of 2016 IEEE Information Technology, Networking, Electronic and Automation Control Conference, ITNEC 2016*, 132–136. <https://doi.org/10.1109/ITNEC.2016.7560334>.
126. Qi, D., & Majda, A. J. (20). Using machine learning to predict extreme events in complex systems. *Proceedings of the National Academy of Sciences of the United States of America*, 117(1), 52–59. <https://doi.org/10.1073/pnas.1917285117>.
127. Qin, H., Li, X., Liang, J., Peng, Y., Zhang, C., 2016. DeepFish: Accurate underwater live fish recognition with a deep architecture. *Neurocomputing* 187, 49–58. doi:10.1016/j.neucom.2015.10.122
128. Racault, M.-F., Platt, T., Sathyendranath, S., A irba , E., Martinez Vicente, V., Brewin, R., 2014. Plankton indicators and ocean observing systems: Support to the Marine Ecosystem State Assessment. *Journal of Plankton Research* 36, 621–629. doi:10.1093/plankt/fbu016.
129. Raphael, A., Dubinsky, Z., Iluz, D., Benichou, J. I. C., & Netanyahu, N. S. (2020). Deep neural network recognition of shallow water corals in the Gulf of Eilat (Aqaba).

130. Raven, J., Caldeira, K., Elderfield, H., Hoegh-Guldberg, O., Liss, P., Riebesell, U., ... & Watson, A. 2005. *Ocean acidification due to increasing atmospheric carbon dioxide*. The Royal Society.
131. Roch, M.A., Soldevilla, M.S., Hoenigman, R., Wiggins, S.M. & Hildebrand, J.A. (2008). Comparison of machine learning techniques for the classification of echolocation clicks from three species of odontocetes. *Canadian Acoustics*, 36(1), 41-47. <https://escholarship.org/uc/item/4895m9g5>.
132. Rolke, M., Lenz, J., 1984. Size structure analysis of zooplankton samples by means of an automated image analyzing system. *Journal of Plankton Research* 6, 637–645. doi:10.1093/plankt/6.4.637.
133. Rosso, I., Mazloff, M. R., Talley, L. D., Purkey, S. G., Freeman, N. M., & Maze, G. (2020). Water Mass and Biogeochemical Variability in the Kerguelen Sector of the Southern Ocean: A Machine Learning Approach for a Mixing Hot Spot. *Journal of Geophysical Research: Oceans*, 125 (3). <https://doi.org/10.1029/2019jc015877>.
134. Sabine, C.L., Feely, R.A., Gruber, N., Key, R.M., Lee, K., Bullister, J.L., Wanninkhof, R., Wong, C.S., Wallace, D.W., Tilbrook, B., Millero, F.J., Peng, T.-H., Kozyr, A., Ono, T., Rios, A.F., 2004. The oceanic sink for anthropogenic co₂. *Science* 305, 367–371. doi:10.1126/science.1097403.
135. Sadaippan, B., Kannan, S., Palaniappan, S., Manikkam, R., Ramasamy, B., Anilkumar N., & Subramanian, M. 2020. Metagenomic 16S rDNA amplicon data of microbial diversity and its predicted metabolic functions in the Southern Ocean (Antarctic). In *Data in Brief* (Vol. 28, p. 104876). Elsevier BV. <https://doi.org/10.1016/j.dib.2019.104876>.
136. Sadaippan, B., PrasannaKumar, C., Nambiar, V. U., Subramanian, M., & Gauns, M. U. (2021). Meta-analysis cum machine learning approaches address the structure and biogeochemical potential of marine copepod associated bacteriobiomes. *Scientific Reports*, 11(1), 1–17. <https://doi.org/10.1038/s41598-021-82482-z>.
137. Sadaippan, B., Prasannakumar, C., Subramanian, K., & Subramanian, M. 2019. Metagenomic data of vertical distribution and abundance of bacterial diversity in the hypersaline sediments of Mad Boon-mangrove ecosystem, Bay of Bengal. In *Data in Brief* (Vol. 22, pp. 716–721). Elsevier BV. <https://doi.org/10.1016/j.dib.2018.12.028>.

138. Saleh, A., Laradji, I. H., Konovalov, D. A., Bradley, M., Vazquez, D., & Sheaves, M. (2020). A realistic fish-habitat dataset to evaluate algorithms for underwater visual analysis. *Scientific Reports*, 10(1), 1–10. <https://doi.org/10.1038/s41598-020-71639-x>.
139. Sarma, V.V., 2003. Monthly variability in surface pCO₂ and net air-sea CO₂ flux in the Arabian Sea. *Journal of Geophysical Research* 108. doi:10.1029/2001jc001062
140. Sarma, V.V., Saino, T., Sasaoka, K., Nojiri, Y., Ono, T., Ishii, M., Inoue, H.Y., Matsumoto, K., 2006. Basin-scale PCO₂ distribution using satellite sea surface temperature, CHL_a, and climatological salinity in the North Pacific in spring and Summer. *Global Biogeochemical Cycles* 20. doi:10.1029/2005gb002594
141. Schlimpert, O., Uhlmann, D., Schüller, M., Höhne, E., 1980. Automated pattern recognition of phytoplankton – procedure and results. *Internationale Revue der gesamten Hydrobiologie und Hydrographie* 65, 427–437. doi:10.1002/iroh.19800650311.
142. Schoening, T., Bergmann, M., Ontrup, J., Taylor, J., Dannheim, J., Gutt, J., Purser, A., & Nattkemper, T. W. (2012). Semi-automated image analysis for the assessment of megafaunal densities at the Arctic deep-sea observatory HAUSGARTEN. *PLoS ONE*, 7(6), 1–14 <https://doi.org/10.1371/journal.pone.0038179>.
143. SHI, Z.H.E.N.G.R.U.I., WANG, K.A.I., CAO, L.U.J.I.E., REN, Y.U., HAN, Y.U., MA, S.H.I.X.I.N., 2019. Study on holographic image recognition technology of Zooplankton. *DEStech Transactions on Computer Science and Engineering*. doi:10.12783/dtsc/cisnrc2019/33361
144. Shiu, Y., Palmer, K. J., Roch, M. A., Fleishman, E., Liu, X., Nosal, E. M., Helble, T., Cholewiak, D., Gillespie, D., & Klinck, H. (2020). Deep neural networks for automated detection of marine mammal species. *Scientific Reports*, 10(1), 1–12. <https://doi.org/10.1038/s41598-020-57549-y>
145. Simpson R, Culverhouse PF, Ellis R, Willaims R (1991) Classification of Euceratium Gran. in neural networks. *IEEE International Conference on Neural Networks in Ocean Engineering*, Washington, DC, USA, August 1991. IEEE, Piscataway, NJ, p 223–230.
146. Sosik, H. M., & Olson, R. J. (2007). Automated taxonomic classification of phytoplankton sampled with imaging-in-flow cytometry. *Limnology and Oceanography: Methods*, 5(6), 204–216. <https://doi.org/10.4319/lom.2007.5.204>.
147. Stephens, M.P., Samuels, G., Olson, D.B., Fine, R.A., Takahashi, T., 1995. Sea-air flux of CO₂ in the North Pacific using shipboard and satellite data. *Journal of Geophysical Research* 100, 13571. doi:10.1029/95jc00901

148. Su, H., Yang, X., & Yan, X. H. (2019). Estimating Ocean Subsurface Salinity from Remote Sensing Data by Machine Learning. *International Geoscience and Remote Sensing Symposium (IGARSS)*, 8139–8142. <https://doi.org/10.1109/IGARSS.2019.8898899>.
149. Sun, M., Cai, Y., Zhang, K., Zhao, X., & Chen, Z. (2020). A method to analyze the sensitivity ranking of various abiotic factors to acoustic densities of fishery resources in the surface mixed layer and bottom cold water layer of the coastal area of low latitude: a case study in the northern South China Sea. *Scientific Reports*, 10(1), 1–13. <https://doi.org/10.1038/s41598-020-67387-7>.
150. Tamou, A.B., Benzinou, A., Nasreddine, K., Ballihi, L., 2018. Underwater live fish recognition by Deep Learning. *Lecture Notes in Computer Science* 275–283. doi:10.1007/978-3-319-94211-7_30 .
151. Tang X (1998) Multiple competitive learning network fusion for object classification. *IEEE T Syst Man Cy* B28:532–543.
152. Tang X, Stewart WK, Vincent L, Huang H, Marra M, Gallager SM, Davis CS (1998) Automatic plankton image recognition. *Artif Intell Rev* 12:177–199.
153. Tang, W., Li, Z., & Cassar, N. (2019). Machine Learning Estimates of Global Marine Nitrogen Fixation. *Journal of Geophysical Research: Biogeosciences*, 124(3), 717–730. <https://doi.org/10.1029/2018JG004828>.
154. Thode, A., Mellinger, D.K., Stienessen, S., Martinez, A., Mullin, K., 2002. Depth-dependent acoustic features of diving sperm whales (*physeter macrocephalus*) in the Gulf of Mexico. *The Journal of the Acoustical Society of America* 112, 308–321. doi:10.1121/1.1482077
155. Thomas, M. K., Fontana, S., Reyes, M., & Pomati, F. (2018). Quantifying cell densities and biovolumes of phytoplankton communities and functional groups using scanning flow cytometry, machine learning and unsupervised clustering. *PLoS ONE*, 13(5), 1–22. <https://doi.org/10.1371/journal.pone.0196225>.
156. Todorovski, L., Džeroski, S., & Kompare, B. (1998). Modelling and prediction of phytoplankton growth with equation discovery. *Ecological Modelling*, 113(1–3), 71–81. [https://doi.org/10.1016/S0304-3800\(98\)00135-5](https://doi.org/10.1016/S0304-3800(98)00135-5).
157. Tyrrell, T. (1999). The relative influences of nitrogen and phosphorus on oceanic primary production. *Nature*, 400(6744), 525–531. <https://doi.org/10.1038/22941>.
158. Valera, M., Walter, R. K., Bailey, B. A., & Castillo, J. E. (2020). Machine Learning Based Predictions of Dissolved Oxygen in a Small Coastal Embayment. *Journal of Marine Science and Engineering*, 8(12), 1007. <https://doi.org/10.3390/jmse8121007>.

159. Van der Schaar, M., Delory, E., Català, A., & André, M. (2007). Neural network-based sperm whale click classification. In *Journal of the Marine Biological Association of the United Kingdom* (Vol. 87, Issue 1, pp. 35–38). Cambridge University Press (CUP). <https://doi.org/10.1017/s0025315407054756>.
160. Villon, S., Mouillot, D., Chaumont, M., Subsol, G., Claverie, T., & Villéger, S. (2020). A new method to control error rates in automated species identification with deep learning algorithms. *Scientific Reports*, 10(1). <https://doi.org/10.1038/s41598-020-67573-7>.
161. Volf, G., Kompare, B., & Ožanić, N. (2014). Use of machine learning for determining phytoplankton dynamic on station RV001 in front of Rovinj (Northern Adriatic). *Engineering Review*, 34(3), 181–187.
162. Voss, M., Bange, H. W., Dippner, J. W., Middelburg, J. J., Montoya, J. P., & Ward, B. (2013). The marine nitrogen cycle: recent discoveries, uncertainties and the potential relevance of climate change. *Philosophical Transactions of the Royal Society B: Biological Sciences*, 368(1621), 20130121. <https://doi.org/10.1098/rstb.2013.0121>.
163. Wang, L., Jiang, Y., & Qi, H. (2020). Marine Dissolved Oxygen Prediction With Tree Tuned Deep Neural Network. In *IEEE Access* (Vol. 8, pp. 182431–182440). Institute of Electrical and Electronics Engineers (IEEE).
164. Wang, S., Kinnison, D., Montzka, S. A., Apel, E. C., Hornbrook, R. S., Hills, A. J., Blake, D. R., Barletta, B., Meinardi, S., Sweeney, C., Moore, F., Long, M., Saiz-Lopez, A., Fernandez, R. P., Tilmes, S., Emmons, L. K., & Lamarque, J. F. (2019). Ocean Biogeochemistry Control on the Marine Emissions of Brominated Very Short-Lived Ozone-Depleting Substances: A Machine-Learning Approach. *Journal of Geophysical Research: Atmospheres*, 124(22), 12319–12339. <https://doi.org/10.1029/2019JD031288>.
165. Weber, T., Wiseman, N. A., & Kock, A. (2019). Global ocean methane emissions dominated by shallow coastal waters. *Nature Communications*, 10(1), 1–10. <https://doi.org/10.1038/s41467-019-12541-7>.
166. Xiao, Z., Peng, L., Chen, Y., Liu, H., Wang, J., & Nie, Y. (2017). The dissolved oxygen prediction method based on a neural network. *Complexity*, 1-6. <https://doi.org/10.1155/2017/4967870>.
167. Xiu Li, Zuoying Cui, 2016. Deep residual networks for plankton classification. OCEANS 2016 MTS/IEEE Monterey. doi:10.1109/oceans.2016.7761223.
168. Xiu Li, Zuoying Cui, 2016. Deep residual networks for plankton classification. OCEANS 2016 MTS/IEEE Monterey, pp. 1-4. doi:10.1109/oceans.2016.7761223

169. Yang, H., An, Z., Zhou, H., & Hou, Y. (2018). Application of machine learning methods in bioinformatics. *AIP Conference Proceedings*, 1967(May). <https://doi.org/10.1063/1.5039089>.
170. Ye, L., Chang, C.Y., Hsieh, C., 2011. Bayesian model for semi-automated zooplankton classification with predictive confidence and rapid category aggregation. *Marine Ecology Progress Series* 441, 185–196. doi:10.3354/meps09387.
171. Yi, H. S., Lee, B., Park, S., Kwak, K. C., & An, K. G. (2019). Prediction of short-term algal bloom using the M5P model-tree and extreme learning machine. *Environmental Engineering Research*, 24(3), 404–411. <https://doi.org/10.4491/EER.2018.245>.
172. Yñiguez, A. T., & Ottong, Z. J. (2020). Predicting fish kills and toxic blooms in an intensive mariculture site in the Philippines using a machine learning model. In *Science of The Total Environment* (Vol. 707, p. 136173). Elsevier BV. <https://doi.org/10.1016/j.scitotenv.2019.136173>.
173. Yu, X., Shen, J., & Du, J. (2020). A Machine-Learning-Based Model for Water Quality in Coastal Waters, Taking Dissolved Oxygen and Hypoxia in Chesapeake Bay as an Example. In *Water Resources Research* (Vol. 56, Issue 9). American Geophysical Union (AGU). <https://doi.org/10.1029/2020wr027227>.
174. Zeng, J., Matsunaga, T., Saigusa, N., Shirai, T., Nakaoka, S. I., & Tan, Z. H. (2017). Evaluation of three machine learning models for surface ocean CO₂ mapping. *Ocean Science*, 13(2), 303–313. <https://doi.org/10.5194/os-13-303-2017>.
175. Zeng, J., Matsunaga, T., Saigusa, N., Shirai, T., Nakaoka, S.-ichiro, Tan, Z.-H., 2017. Technical note: Evaluation of three machine learning models for Surface Ocean CO₂ mapping. *Ocean Science* 13, 303–313. doi:10.5194/os-13-303-2017.
176. Zeng, J., Nojiri, Y., Nakaoka, S., Nakajima, H., Shirai, T., 2015. Surface ocean CO₂ in 1990–2011 modelled using a feed-forward neural network. *Geoscience Data Journal* 2, 47–51. doi:10.1002/gdj3.26.
177. Zheng, H., Wang, R., Yu, Z., Wang, N., Gu, Z., & Zheng, B. (2017). Automatic plankton image classification combining multiple view features via multiple kernel learning. *BMC Bioinformatics*, 18(238), 1–18. <https://doi.org/10.1186/s12859-017-1954-8>.
178. Zhong, G., Li, X., Song, J., Qu, B., Wang, F., Wang, Y., Zhang, B., Sun, X., Zhang, W., Wang, Z., Ma, J., Yuan, H., Duan, L., 2022. Reconstruction of Global Surface Ocean pCO₂ using region-specific predictors based on a stepwise FFNN regression algorithm. *Biogeosciences* 19, 845–859. doi:10.5194/bg-19-845-2022.

179. Zhu, Y., Shang, S., Zhai, W., Dai, M., 2009. Satellite-derived surface water PCO₂ and air–sea CO₂ fluxes in the northern South China Sea in Summer. *Progress in Natural Science* 19, 775–779. doi:10.1016/j.pnsc.2008.09.004
180. Zieger, S. E., Seoane, S., Laza-Martínez, A., Knaus, A., Mistlberger, G., & Klimant, I. (2018). Spectral Characterization of Eight Marine Phytoplankton Phyla and Assessing a Pigment-Based Taxonomic Discriminant Analysis for the *in situ* Classification of Phytoplankton Blooms. *Environmental Science and Technology*, 52(24), 14266–14274. <https://doi.org/10.1021/acs.est.8b04528>.